

Risk reversal for least squares estimators under nested convex constraints

Omar Al-Ghattas

Broad Institute of MIT and Harvard

Abstract

In constrained stochastic optimization, one naturally expects that imposing a stricter feasible set does not increase the statistical risk of an estimator defined by projection onto that set. In this paper, we show that this intuition can fail even in canonical settings.

We study the Gaussian sequence model, a canonical test bed that offers a deliberately austere setting for the phenomenon considered here, where for a compact, convex set $\Theta \subset \mathbb{R}^d$ one observes

$$Y = \theta^* + \sigma Z, \quad Z \sim N(0, I_d),$$

and seeks to estimate an unknown parameter $\theta^* \in \Theta$. The natural estimator in this setting is the least squares estimator (LSE), which coincides with the Euclidean projection of Y onto Θ . We construct an explicit example exhibiting *risk reversal*: for sufficiently large noise, there exist nested compact convex sets $\Theta_S \subset \Theta_L$ and a parameter $\theta^* \in \Theta_S$ such that the LSE constrained to Θ_S has strictly larger risk than the LSE constrained to Θ_L . Moreover, we demonstrate that risk reversal can persist at the level of worst-case risk, in the sense that the supremum of the risk over the smaller constraint set exceeds that over the larger one.

We clarify this phenomenon by contrasting the behavior of the LSE across noise regimes. In the vanishing-noise limit, the risk admits a first-order expansion governed by the statistical dimension of the tangent cone at θ^* , and risk reversal cannot occur: tighter constraints uniformly reduce risk. In contrast, in the diverging-noise regime, the risk is determined by global geometric interactions between the constraint set and random noise directions. Here, the embedding of Θ_S within Θ_L , rather than the local geometry at θ^* , plays a decisive role in the behavior of the LSE and can reverse the risk ordering.

These results reveal a previously unrecognized failure mode of the LSE, and of projection-based estimators more broadly. They demonstrate that in sufficiently noisy settings, tightening a constraint can paradoxically degrade statistical performance.

1 Introduction

In statistical estimation, it is standard to analyze estimators under the assumption that the unknown parameter belongs to a prescribed feasible set. Such constraints encode prior structural information, reduce the effective complexity of the parameter space, and are therefore widely believed to improve estimation accuracy. This perspective naturally fosters the intuition that, when a constraint is correctly specified, further restricting the feasible set in a way that preserves the truth should not worsen performance.

In applied work, constraints rarely appear fully formed. More often, a statistician begins with a simple modeling assumption, such as boundedness or smoothness, and then gradually refines the model as additional insight becomes available. New constraints may be introduced to reflect domain knowledge, improve interpretability, or enforce desired qualitative behavior. Each refinement is typically viewed as a step toward a more faithful representation of the underlying problem, and thus toward better statistical performance. From this perspective, it is far from obvious that adding valid structure could ever worsen statistical performance.

We study this question in the Gaussian sequence model, one of the simplest and most benign settings for constrained estimation, under well-behaved (namely, compact and convex) constraints. As we will argue, this model also provides a deliberately austere setting in which to exhibit the phenomenon we

identify. Here, the natural estimator is the least squares estimator (LSE), which coincides with the maximum likelihood estimator and admits a geometric characterization as the Euclidean projection onto the constraint set. Although this formulation is canonical, existing analyses of the LSE typically rely on local approximations near the true parameter and therefore do not capture how the estimator's risk depends on the global geometry of the constraint set. When two compact, convex constraint sets are nested and the smaller set contains the true parameter, one might expect the corresponding LSE to have lower risk. We show that this intuition can fail: there exist settings in which the LSE associated with the smaller constraint has strictly larger risk than that associated with the larger constraint, both pointwise at a fixed parameter and at the level of worst-case risk.

1.1 Problem Setup

We now introduce the mathematical framework that will serve as the basic object of study throughout the paper. Let $\Theta_S, \Theta_L \subset \mathbb{R}^d$ be compact, convex sets satisfying

$$\Theta_S \subset \Theta_L,$$

and suppose the unknown parameter θ^* lies in Θ_S . We observe a single realization from the Gaussian sequence model

$$Y = \theta^* + \sigma Z, \quad Z \sim N(0, I_d), \quad (1)$$

where $\sigma > 0$ denotes the noise level. Our goal is to estimate θ^* from the noisy observation Y .

For a compact, convex set $\Theta \subset \mathbb{R}^d$, define the Euclidean projection of a point $y \in \mathbb{R}^d$ onto Θ by

$$\Pi_\Theta(y) := \arg \min_{\theta \in \Theta} \|y - \theta\|^2.$$

Since Θ is compact and convex, the minimizer exists and is unique. The estimator $\Pi_\Theta(Y)$ is the LSE, which coincides with the maximum likelihood estimator under the constraint $\theta^* \in \Theta$.

We consider the two LSEs

$$\hat{\theta}_S := \Pi_{\Theta_S}(Y), \quad \hat{\theta}_L := \Pi_{\Theta_L}(Y),$$

and evaluate their performance using the squared-error risk

$$R_\sigma(\theta^*; \Theta) := \mathbb{E}_{\theta^*} \|\hat{\theta} - \theta^*\|^2.$$

Throughout the paper, the notation $R_\sigma(\theta^*; \Theta)$ always denotes the risk of the estimator $\Pi_\Theta(\theta^* + \sigma Z)$. The inclusion $\Theta_S \subset \Theta_L$ suggests a natural comparison. The estimator $\hat{\theta}_S$ enforces a stronger constraint and thus incorporates more prior information than $\hat{\theta}_L$, while remaining correctly specified whenever $\theta^* \in \Theta_S$. This leads to the central question of this work: can strengthening the constraint ever increase the estimation risk? In particular, do there exist settings in which

$$R_\sigma(\theta^*; \Theta_S) > R_\sigma(\theta^*; \Theta_L),$$

a phenomenon we refer to as *risk reversal*. Beyond this pointwise comparison, we also ask whether an analogous reversal can occur at the level of worst-case risk over the constraint set.

Remark 1.1 (Multiple observations). Throughout this work we state results for a single observation of (1) only for notational simplicity and without loss of generality. If instead one observes $n \geq 1$ independent samples $Y_1, \dots, Y_n \sim N(\theta^*, \sigma^2 I_d)$, the LSE is simply the orthogonal projection of the sample mean \bar{Y} onto the constraint set. Since \bar{Y} is Gaussian with mean θ^* and variance $\frac{\sigma^2}{n} I_d$, the n sample problem is exactly equivalent to the single-sample model with effective noise level $\frac{\sigma}{\sqrt{n}}$. In particular, all diverging-noise results of this paper continue to hold verbatim whenever the effective noise level diverges. \square

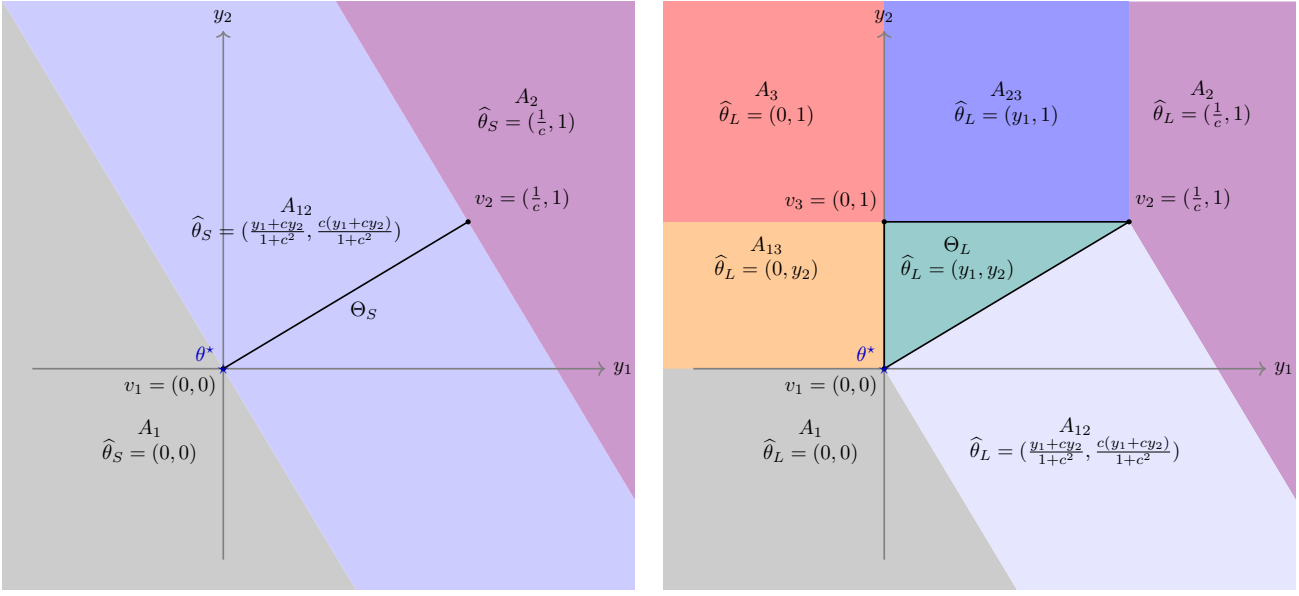


Figure 1 Geometry of the LSE over constraint sets $\Theta_S = \text{conv}(v_1, v_2)$ (left) and $\Theta_L = \text{conv}(v_1, v_2, v_3)$ (right). The shaded regions illustrate the partition of the sample space based on the location of the constrained solution: regions A_j denote observations projected onto vertex v_j , while regions A_{ij} denote observations projected onto the line segment connecting v_i and v_j .

1.2 Risk reversal: an explicit example

We now describe the core phenomenon identified in this work by constructing a concrete example in which risk reversal occurs. Specifically, we construct a simple two-dimensional example in the Gaussian sequence model in which the risk of the projection estimator under a tighter, correctly specified constraint exceeds that under a looser constraint. The example admits explicit expressions for the risks associated with both constraints, allowing us to examine in detail how the risk depends on the noise level σ . These calculations reveal a nontrivial interaction between noise and global constraint geometry, and motivate the more systematic analysis of the small- and diverging-noise regimes carried out in subsequent sections. While the results of this paper ultimately establish a stronger form of risk reversal—showing that the phenomenon can persist even at the level of worst-case risk over the constraint set—the pointwise example presented here plays a central conceptual role. It isolates the geometric mechanism by which risk reversal arises and provides concrete intuition for how global misalignment between nested constraints can lead to counterintuitive behavior of the LSE, thereby guiding the general asymptotic framework developed later in the paper.

Example 1.1. Fix a constant $c > 0$ and define the points

$$v_1 := (0, 0), \quad v_2 := \left(\frac{1}{c}, 1\right), \quad v_3 := (0, 1).$$

Let

$$\Theta_L := \text{conv}\{v_1, v_2, v_3\}$$

denote the convex hull of these points, forming a closed triangular region, and let

$$\Theta_S := \text{conv}\{v_1, v_2\}$$

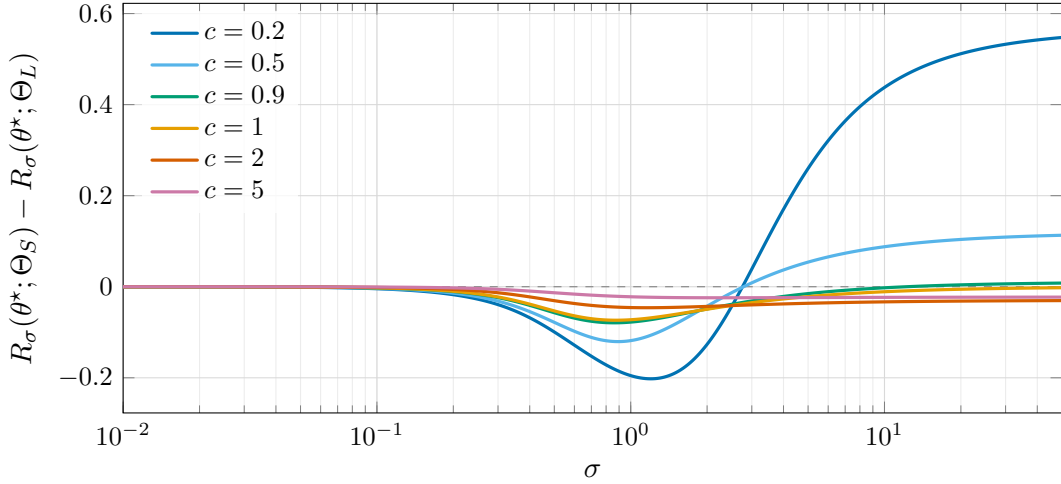


Figure 2 Risk difference as a function of noise level σ . The difference $R_\sigma(\theta^*; \Theta_S) - R_\sigma(\theta^*; \Theta_L)$ is plotted against σ for varying values of the geometric parameter c . Note that for $c \in \{0.2, 0.5, 0.9\}$, $\hat{\theta}_L$ outperforms $\hat{\theta}_S$ whenever the noise level is sufficiently large.

denote the line segment joining v_1 and v_2 . We observe a single realization from the Gaussian sequence model (1) with true parameter $\theta^* = v_1$. Let $\hat{\theta}_S$ and $\hat{\theta}_L$ denote the corresponding LSEs under the constraints Θ_S and Θ_L , respectively.

Note that the choice $\theta^* = v_1$ is without loss of generality, since one may translate the constraint sets so that the true parameter lies at the origin. We depict the constraint sets and the action of the LSEs across different regions of the sample space in Figure 1.

Theorem 1.2. Consider the setting of Example 1.1. For any $\sigma > 0$, the risks $R_\sigma(\theta^*; \Theta_S)$ and $R_\sigma(\theta^*; \Theta_L)$ admit exact closed-form representations. Moreover, the following asymptotic comparisons hold.

(i) *Vanishing-noise regime.* As $\sigma \rightarrow 0^+$,

$$R_\sigma(\theta^*; \Theta_S) - R_\sigma(\theta^*; \Theta_L) = -\frac{\sigma^2}{\pi} \arctan \frac{1}{c} + o(\sigma^2). \quad (2)$$

In particular, there exists $\sigma_0 > 0$ such that for all $\sigma \in (0, \sigma_0)$,

$$R_\sigma(\theta^*; \Theta_S) < R_\sigma(\theta^*; \Theta_L).$$

(ii) *Diverging-noise regime.* As $\sigma \rightarrow \infty$,

$$R_\sigma(\theta^*; \Theta_S) - R_\sigma(\theta^*; \Theta_L) = \frac{1}{4c^2} - \frac{1+c^2}{2\pi c^2} \arctan \frac{1}{c} + o(1). \quad (3)$$

In particular, there exists $\sigma_1 < \infty$ such that for all $\sigma \in (\sigma_1, \infty)$,

$$\begin{cases} R_\sigma(\theta^*; \Theta_S) > R_\sigma(\theta^*; \Theta_L), & 0 < c < 1, \\ R_\sigma(\theta^*; \Theta_S) = R_\sigma(\theta^*; \Theta_L), & c = 1, \\ R_\sigma(\theta^*; \Theta_S) < R_\sigma(\theta^*; \Theta_L), & c > 1. \end{cases}$$

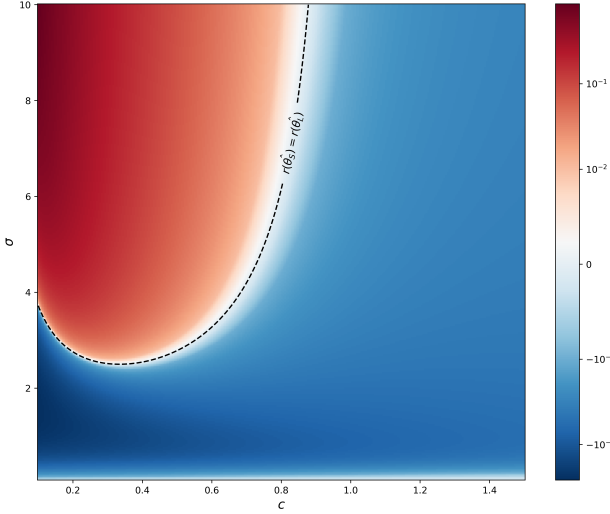


Figure 3 Heat map of the risk difference $R_\sigma(\theta^*; \Theta_S) - R_\sigma(\theta^*; \Theta_L)$ as a function of the geometric parameter c (horizontal axis) and the noise level σ (vertical axis). Risk reversal occurs in a substantial intermediate-to-large noise regime for values of $c \in (0, 1)$.

The proof of Theorem 1.2 and of all other results is given in Section 3.

We emphasize that the key geometric mechanism underlying risk reversal in this example is the misalignment between the larger constraint set Θ_L and the smaller set Θ_S . Although $\Theta_S \subset \Theta_L$, the orientation of Θ_S within Θ_L is such that, for certain realizations of Y , projection onto Θ_S yields an estimate that lies farther from θ^* than the projection onto Θ_L . Figure 4 highlights the subset $\mathcal{G} \subset \mathbb{R}^2$ of points for which this pointwise reversal occurs. This observation reinforces that risk reversal is inherently a non-local phenomenon: it arises from the behavior of the projection map on regions of the sample space away from θ^* and is therefore invisible to geometric characterizations that depend solely on the local structure of the constraint near θ^* . For this pointwise discrepancy to translate into a reversal of risks, it is further necessary that the isotropic Gaussian distribution centered at θ^* assigns non-negligible probability mass to these regions.

Theorem 1.2 shows that, for our specific example, in the vanishing-noise regime, risk reversal cannot occur for all sufficiently small σ . In contrast, the diverging-noise regime is more subtle. Depending on the parameter c , which controls the length of the edge connecting vertices v_2 and v_3 in Θ_L , the risk ordering may either agree with or reverse the vanishing-noise case. In particular, for $0 < c < 1$ the tighter constraint Θ_S has strictly larger risk for sufficiently large σ , whereas for $c > 1$, the ordering is preserved.

The explicit risk expressions enable us to plot the associated risk curves (Figure 2), offering further intuition about the dependence of risk reversal on the noise level. Notably, these curves suggest a monotone behavior in σ , in the sense that once risk reversal occurs, it persists rather than oscillating as σ increases. This observation motivates an analysis of the diverging-noise regime, since the ordering of the risks stabilizes and can be characterized asymptotically. Similarly, we are able to compute risk comparisons across a range of (c, σ) values in Figure 3, which visualizes the difference $R_\sigma(\theta^*; \Theta_S) - R_\sigma(\theta^*; \Theta_L)$ across a range of noise levels σ and geometric configurations indexed by c , demonstrating that risk reversal can take place for moderate to large values of σ .

1.3 Risk reversal: beyond pointwise comparisons

Up to this point, our analysis has focused on a *pointwise* manifestation of risk reversal. One might reasonably view such pointwise failures as relatively mild. Indeed, statistical theory contains many examples—most famously the Hodges super-efficient estimator [VdV00, Chapter 8]—in which an estimator behaves anomalously at isolated points or in small neighborhoods, without representing a genuine global phenomenon. From this perspective, one could ask whether risk reversal is merely a local pathology, in which a tighter constraint degrades performance only at isolated points while still offering uniformly better performance overall, or whether it reflects a more substantial breakdown of the LSE.

A natural way to strengthen the comparison is to consider the worst-case risk over the constraint set. From a decision-theoretic perspective, this corresponds to evaluating the estimator under the least favorable parameter consistent with the assumed constraint. If tightening a correctly specified constraint increases even the worst-case risk, then the phenomenon cannot be dismissed as localized or atypical.

Theorem 1.3. *There exist nested, compact, and convex sets $\Theta_S \subset \Theta_L$ such that there exists $\sigma_1 < \infty$ with the property that for all $\sigma \in (\sigma_1, \infty)$,*

$$\sup_{\theta \in \Theta_S} R_\sigma(\theta; \Theta_S) > \sup_{\theta \in \Theta_L} R_\sigma(\theta; \Theta_L).$$

Theorem 1.3 follows immediately by Lemma 2.12, which in turn relies on a characterization of the LSE in the diverging-noise regime developed in Section 2.2. In particular, we construct explicit constraint sets whose limiting risks exhibit worst-case risk reversal as $\sigma \rightarrow \infty$. We then show that, in this regime, the risk function converges uniformly over the constraint set. As a consequence, worst-case risk reversal must already occur at some finite noise level. We provide a detailed description of the result in Section 2.2.2.

Remark 1.4 (Gaussian sequence model as a conservative testbed). At first glance, the phenomena exhibited in this work may appear to be an artifact of the Gaussian sequence model (1). We emphasize, however, that this model represents a particularly stringent setting in which to demonstrate risk reversal, and that our results point to the broader relevance of the phenomenon beyond this special case.

First, in our setting, the LSE coincides with the maximum likelihood estimator: it is the maximizer of the Gaussian likelihood over Θ . Thus, the procedure we study is the canonical likelihood-based estimator under the assumed constraint, rather than an ad hoc construction, so any observed degradation in risk reflects a genuine feature of projection-based estimation. Moreover, throughout our examples the constraint sets are correctly specified, in the sense that $\theta^* \in \Theta_S \subset \Theta_L$, so risk reversal does not arise from model misspecification.

Second, the noise in the Gaussian sequence model is light-tailed, which severely limits the extent to which probability mass can concentrate in regions of the sample space that favor the larger constraint relative to the smaller one. In contrast, heavy-tailed noise introduces qualitatively different behavior and redistributing mass toward such regions can more easily induce risk reversal. Figure 4 illustrates that even modest departures from Gaussianity would substantially simplify the construction of such examples.

Third, we focus on compact, convex constraint sets, under which the projection estimator is well defined and the large-noise behavior admits a clean geometric characterization. Compactness ensures that the estimator’s asymptotic behavior is governed by the selection of exposed faces via supporting hyperplanes (see Section 2.2), rather than by movement along unbounded directions of the constraint set. While extending the analysis to unbounded constraint sets would require additional control of such directions, the examples considered here already demonstrate that risk reversal can arise even under these restrictive and well-behaved assumptions.

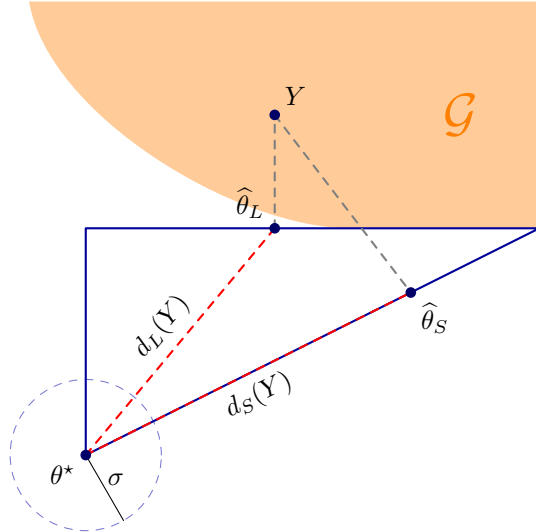


Figure 4 A schematic illustration of the risk reversal phenomenon. A realization Y is projected onto the larger constraint set, yielding $\hat{\theta}_L$, and onto the smaller set, yielding $\hat{\theta}_S$. In this configuration, the distance from θ^* of projecting onto the larger set, $d_L(Y) = \|\Pi_{\Theta_L}(Y) - \theta^*\|$, is smaller than the corresponding distance of projecting onto the smaller set, $d_S(Y) = \|\Pi_{\Theta_S}(Y) - \theta^*\|$. The shaded region denotes the set $\mathcal{G} = \{y : d_L(y) < d_S(y)\}$ of all points for which projecting on to the small set is relatively worse. When the noise level σ is sufficiently large, the Gaussian centered at θ^* places enough mass on \mathcal{G} for the risk associated with projection onto Θ_L to be smaller than that associated with projection onto Θ_S .

Although some of our theoretical analysis is asymptotic in nature, the phenomenon of risk reversal itself is not: we demonstrate that it occurs at finite noise levels, with the asymptotic regime serving primarily as a mathematically tractable lens for isolating and clarifying the underlying mechanism. Moreover, the effect arises in fixed dimension and for a single observation, rather than relying on high-dimensional asymptotics or other limiting regimes.

For these reasons, we view the Gaussian sequence model not as a restrictive special case, but as a conservative testbed in which any instance of risk reversal must arise from intrinsically global geometric interactions between constraint sets. \square

1.4 Related literature

Estimating the mean of a noisy vector under Gaussian noise, known in statistics as the *Gaussian sequence model* and in signal processing as *Gaussian denoising*, is among the most classical problems in these fields, and the literature on this topic is correspondingly vast. We refer the reader to the monographs [Joh19, Tsy09] and the references therein for comprehensive treatments.

A major advance in understanding the risk of the LSE was made in the seminal work of [Cha14], which provided the first two-sided, pointwise characterization of the risk over general closed, convex constraint sets. That work also established that, although the LSE is not minimax optimal in general, it nevertheless satisfies a form of admissibility. Moreover, [Cha14] emphasized the Gaussian sequence model as a unifying abstraction, encompassing prominent estimators such as the LASSO and isotonic regression.

Complementary lines of work have highlighted the role of convex and conic geometry in governing the risk of the LSE. In particular, [OH16] characterized the vanishing-noise risk of the LSE in terms of

the statistical dimension of the tangent cone at the true parameter. The foundational role of statistical dimension and related geometric quantities was subsequently formalized in the influential work of [ALMT14], which established sharp phase transition phenomena for the related Gaussian linear measurement model with random Gaussian design. Closely related ideas underlie precise risk analyses for broader classes of estimators, including generalized LASSO and proximal denoising procedures; see, for example, [OTH13]. More recently, these geometric techniques have been extended to obtain exact risk characterizations in the high-dimensional asymptotic for the LSE in the Gaussian linear measurement model [Han23].

Despite this extensive body of work, the risk reversal phenomenon studied in this paper—where enlarging a convex constraint set leads to a decrease in risk—has not, to the best of our knowledge, been previously investigated. Existing analyses of the constrained LSE have primarily focused on suboptimality from a minimax perspective; see, for instance, the recent works [PN25, AJPU25, Ney23] and the discussions therein. Important works in this area include [BM93, KRG20, KPR23, KGGS24, Zha13, WFW20]. In contrast, our results reveal a qualitatively different failure mode that is invisible to minimax theory and persists even when both constraint sets are well-specified.

One work that reports a surprising, though conceptually distinct, phenomenon is [FG19]. There, the authors show that for polyhedral constraint sets, the normalized risk of the constrained LSE can be smaller in the misspecified setting, when the true parameter lies outside the constraint set, than in the well-specified case. This behavior is driven by misspecification bias and should be contrasted with the present work, which concerns well-specified models and nested constraint sets.

Finally, we note a separate line of work—unrelated to the focus of this paper—that studies a different notion of *risk monotonicity* [BDK⁺22, MH20, VML20], concerned with how risk evolves as the sample size increases. This notion should not be confused with the risk reversal phenomenon considered here, which arises from geometric effects under fixed sample size and varying constraint sets.

1.4.1 Chatterjee's risk characterization

The work of [Cha14] provides the most general and influential characterization of the risk of the constrained LSE in the Gaussian sequence model. Given its scope and sharpness, it is natural to ask whether Chatterjee's framework can detect, or rule out, the risk reversal phenomenon studied in this paper. We briefly explain why it likely cannot. [Cha14] states their results in the unit-noise model (i.e. $Y = \theta^* + Z$, $Z \sim N(0, I_d)$), and studies the LSE $\hat{\theta} = \Pi_\Theta(Y)$, where $\Theta \subset \mathbb{R}^d$ is closed and convex. [Cha14, Corollary 1.2] relates the risk to a single scale parameter t_θ , defined as the unique maximizer of the function

$$f_\theta(t) = \mathbb{E} \left[\sup_{\nu \in \Theta: \|\nu - \theta\| \leq t} \langle Z, \nu - \theta \rangle \right] - \frac{t^2}{2}.$$

In the regime $t_\theta \geq 1$, [Cha14, Corollary 1.2] yields a sharp two-sided characterization of the risk,

$$\mathbb{E}_\theta \|\hat{\theta} - \theta\|^2 = t_\theta^2 + O(t_\theta^{3/2}),$$

revealing that the risk is governed by the local Gaussian complexity of Θ near θ . When $t_\theta < 1$, however, the conclusion becomes substantially weaker: the corollary guarantees only that the risk is bounded by a universal constant. In the general noise model, application of [Cha14, Corollary 1.2] proceeds by rescaling $\theta' = \frac{\theta}{\sigma}$ and $\Theta' = \frac{\Theta}{\sigma}$, applying the $\sigma = 1$ result to (θ', Θ') , and then multiplying the resulting bound by σ^2 . In cases where Θ is bounded, such as the nested polytopes $\Theta_S \subset \Theta_L$ of Example 1.1, the associated maximizer $t_{\theta'}$ typically lies in the small- t regime across a wide range of σ .

This loss of sharpness can be understood as follows. For bounded Θ , the rescaled set Θ' shrinks as σ increases, so the geometry relevant to $t_{\theta'}$ is that of a small neighborhood of θ' . Let $\text{rad}_\theta(\Theta) :=$

$\sup_{\nu \in \Theta} \|\nu - \theta\|$. Since the supremum in $f_\theta(t)$ saturates once $t \geq \text{rad}_\theta(\Theta)$, the maximizer necessarily satisfies $t_\theta \leq \text{rad}_\theta(\Theta)$. Applied to the rescaled problem, this yields

$$t_{\theta'}(\Theta') \leq \frac{\text{rad}_\theta(\Theta)}{\sigma}.$$

Thus, as soon as σ exceeds the geometric radius of Θ , the optimizer $t_{\theta'}$ must lie below 1, forcing us into its small- t regime. For Example 1.1, one can compute explicitly that

$$t_0\left(\frac{\Theta_S}{\sigma}\right) = \min\left(\frac{1}{\sqrt{2\pi}}, \frac{\|v_2\|}{\sigma}\right) < 1 \quad \text{for all } \sigma > 0,$$

and

$$t_0\left(\frac{\Theta_L}{\sigma}\right) \leq \frac{\max(\|v_2\|, \|v_3\|)}{\sigma},$$

so $t_0(\frac{\Theta_L}{\sigma}) < 1$ whenever σ exceeds a fixed constant depending only on the geometry of Θ_L . In both cases, [Cha14, Corollary 1.2] necessarily yields only a universal $O(\sigma^2)$ risk bound.

Our results suggest that risk reversal emerges only once the noise is sufficiently large for the estimator to “zoom out” and interact with the global geometry of the constraint set. The resulting non-local and directional effects are not captured by the one-parameter summary t_θ . Consequently, Chatterjee’s risk characterization does not appear well suited for detecting or establishing the existence of this phenomenon.

2 Asymptotic risk of the least squares estimator

Motivated by the findings in Section 1.2, we turn to a more systematic investigation of the risk reversal phenomenon. Our goal is to formalize how the risk of the LSE depends on the noise level and the geometry of the constraint set. To this end, we analyze the estimator’s behavior in two complementary asymptotic regimes: the vanishing-noise regime ($\sigma \rightarrow 0^+$) and the diverging-noise regime ($\sigma \rightarrow \infty$).

In the vanishing-noise regime, we show that risk reversal is impossible to leading order in σ as $\sigma \rightarrow 0^+$: shrinking the constraint set cannot increase risk. In contrast, in the diverging-noise regime, we demonstrate that risk reversal can arise much more broadly, extending well beyond the specific example considered in Section 1.2. We leverage this finding to construct an example in which risk reversal occurs in supremum-risk, demonstrating that risk reversal is not merely a pointwise phenomena.

Taken together, these results clarify the regimes in which risk reversal is structurally possible.

2.1 Vanishing-noise regime

The Gaussian sequence model in the vanishing-noise regime has been well studied in the literature, with the asymptotic risk of the LSE fully characterized by Oymak and Hassibi [OH16]. We briefly recall the relevant definitions and results.

For a set $A \subset \mathbb{R}^d$ and a vector $b \in \mathbb{R}^d$, we write \overline{A} for the closure of A and $A - b := \{a - b : a \in A\}$. Let $\Theta \subset \mathbb{R}^d$ be a compact, convex set and let $\theta \in \Theta$. The *tangent cone* of Θ at θ is defined as

$$T_\Theta(\theta) := \overline{\bigcup_{t \geq 0} t(\Theta - \theta)}.$$

Since Θ is compact and convex, $T_\Theta(\theta)$ is a closed convex cone. The *statistical dimension* of this cone is given by

$$\delta(T_\Theta(\theta)) := \mathbb{E}\|\Pi_{T_\Theta(\theta)}(Z)\|^2, \quad Z \sim N(0, I_d).$$

Oymak and Hassibi [OH16, Theorem 3.1] show that, as $\sigma \rightarrow 0^+$,

$$R_\sigma(\theta; \Theta) = \sigma^2 \delta(T_\Theta(\theta)) + o(\sigma^2).$$

In Section 3, we provide a separate, self-contained treatment of this setting in Proposition 3.3, based on a different proof strategy. Our argument relies on classical results on the one-sided directional differentiability of Euclidean projections onto closed convex sets [Zar71]; see also [Nol95, Sha16]. This perspective complements existing analyses and may be of independent interest.

An immediate consequence is that risk reversal cannot occur at order σ^2 as $\sigma \rightarrow 0$.

Theorem 2.1. *Let $\Theta_S \subset \Theta_L$ be compact, convex sets and suppose $\theta^* \in \Theta_S$. Then, as $\sigma \rightarrow 0^+$,*

$$R_\sigma(\theta^*; \Theta_S) \leq R_\sigma(\theta^*; \Theta_L) + o(\sigma^2).$$

Consequently, risk reversal cannot occur for sufficiently small noise levels.

Remark 2.2. For interior points $\theta^* \in \text{int}(\Theta)$, standard asymptotic theory for the maximum likelihood estimator implies that as $\sigma \rightarrow 0^+$

$$\frac{R_\sigma(\theta^*; \Theta)}{\sigma^2} \rightarrow d.$$

Geometrically, the tangent cone of an interior point satisfies $T_\Theta(\theta^*) = \mathbb{R}^d$, since an infinitesimal displacement in any direction remains feasible. Consequently, the associated statistical dimension reduces to

$$\delta(T_\Theta(\theta^*)) = \delta(\mathbb{R}^d) = \mathbb{E}\|Z\|^2 = d.$$

In particular, if $\theta^* \in \text{int}(\Theta_S) \subset \text{int}(\Theta_L)$, then

$$R_\sigma(\theta^*; \Theta_S) \sim R_\sigma(\theta^*; \Theta_L) \quad \text{as } \sigma \rightarrow 0^+.$$

It follows that any strict risk separation between the two estimators must be driven by boundary effects, and cannot occur at interior points in the vanishing-noise regime. \square

We derive the vanishing noise risk for Example 1.1. Instead of a direct asymptotic analysis of the explicit risk derived in Theorem 3.1, we compute the statistical dimension of the tangent cone at $\theta^* = v_1$ for each of Θ_S and Θ_L .

Corollary 2.3. *In the setting of Example 1.1, as $\sigma \rightarrow 0^+$,*

$$\begin{aligned} R_\sigma(\theta^*; \Theta_S) &= \frac{\sigma^2}{2} + o(\sigma^2), \\ R_\sigma(\theta^*; \Theta_L) &= \sigma^2 \left(\frac{1}{2} + \frac{1}{\pi} \arctan \frac{1}{c} \right) + o(\sigma^2). \end{aligned}$$

Consequently, $R_\sigma(\theta^*; \Theta_S) < R_\sigma(\theta^*; \Theta_L) + o(\sigma^2)$.

2.2 Diverging-noise regime

In the preceding section, it was demonstrated that in the vanishing-noise regime, the leading-order term of the LSE risk is determined completely by the statistical dimension, which is monotone under set inclusion. As a consequence, risk reversal must arise from either higher-order or non-local effects. This observation, along with our results in Section 1.2, suggest that the risk reversal phenomenon might inherently be tied to moderate or large noise levels.

In this section, we study the diverging-noise regime, in which the least squares estimator is governed by the global geometry of the constraint set. In this limit, the estimator concentrates on exposed faces of Θ selected by a random direction $U = \frac{Z}{\|Z\|}$, and its asymptotic risk is determined by the position of θ^* relative to these faces. This perspective yields a geometric characterization of the mechanisms that can give rise to risk reversal. We also examine the special case of convex polytopes, for which the asymptotic risk admits an explicit representation in terms of the vertices, thereby generalizing the behavior observed in Section 1.2. This provides the necessary machinery to analyze the worst-case risk reversal, which we describe in Section 2.2.2.

Our first result in this section considers the general setting and provides a diverging-noise characterization of almost sure behavior of the LSE as well as its risk.

Theorem 2.4. *Let $\Theta \subset \mathbb{R}^d$ be nonempty, compact and convex and fix $\theta^* \in \Theta$. Let $Z \sim N(0, I_d)$ and for $\sigma > 0$ define*

$$\hat{\theta}_\sigma := \Pi_\Theta(\theta^* + \sigma Z).$$

Set

$$U := \frac{Z}{\|Z\|}, \quad F_\Theta(u) := \arg \max_{\theta \in \Theta} \langle \theta, u \rangle.$$

Then, almost surely, as $\sigma \rightarrow \infty$,

$$\hat{\theta}_\sigma \rightarrow \Pi_{F_\Theta(U)}(\theta^*), \tag{4}$$

and consequently, for $R_\infty(\theta^*; \Theta) := \mathbb{E} \|\Pi_{F_\Theta(U)}(\theta^*) - \theta^*\|^2$,

$$R_\sigma(\theta^*; \Theta) \rightarrow R_\infty(\theta^*; \Theta). \tag{5}$$

Theorem 2.4 shows that, as $\sigma \rightarrow \infty$, the quadratic penalty in the projection problem becomes negligible relative to the linear term induced by the noise direction U , and the estimator concentrates on the exposed face $F_\Theta(U)$ selected by this random direction. The limiting estimator is therefore obtained by first choosing a face of Θ according to U , and then projecting θ onto that face. This contrasts sharply with the vanishing-noise regime and highlights why risk comparisons in large noise are sensitive to the global embedding of nested constraint sets. We remark that for each direction on the unit sphere $u \in \mathbb{S}^{d-1}$, $F_\Theta(u)$ is a nonempty exposed face of Θ , and hence closed and convex; therefore, there is no ambiguity in the definition of $\Pi_{F_\Theta(U)}(\theta^*)$.

2.2.1 Discrete selection: convex polytopes

We restrict to the setting in which Θ is a convex polytope, that is,

$$\Theta = \text{conv}\{v_1, \dots, v_K\},$$

where $v_1, \dots, v_K \in \mathbb{R}^d$ are finitely many vertices. Beyond the fact that Example 1.1 is of this form, convex polytopes arise ubiquitously as constraint sets in stochastic optimization, including the probability simplex

which encodes non-negativity and unit-sum constraints), ℓ_1 -type constraints that promote sparsity, and more general feasible regions defined by linear inequalities.

Accordingly, we analyze the quantity $F_\Theta(U)$ arising in Theorem 2.4 when Θ is a convex polytope. For this class of constraints, $F_\Theta(U)$ admits an explicit and tractable characterization, enabling us to isolate the geometric mechanisms underlying the phenomena observed in Section 1.2 in a general setting.

Before stating the main result of this section, we introduce some additional notation: let μ_{d-1} denote the $(d-1)$ -dimensional surface measure on the unit sphere \mathcal{S}^{d-1} . The uniform distribution on \mathcal{S}^{d-1} is characterized for any measurable $A \subset \mathcal{S}^{d-1}$ by

$$\mathbb{P}(U \in A) = \frac{\mu_{d-1}(A)}{\mu_{d-1}(\mathcal{S}^{d-1})}.$$

Further, the normal cone of Θ at a vertex v_i is

$$\mathcal{N}_\Theta(v_i) = \left\{ u \in \mathbb{R}^d : \langle u, v_j - v_i \rangle \leq 0 \text{ for all } j = 1, \dots, K \right\}.$$

Lemma 2.5. *Let $\Theta \subset \mathbb{R}^d$ be a nonempty compact convex polytope with vertices v_1, \dots, v_K . There exists a random index $I \in \{1, \dots, K\}$ such that, almost surely,*

$$F_\Theta(U) = \{v_I\}.$$

Consequently, in the diverging-noise regime $\sigma \rightarrow \infty$, almost surely,

$$\hat{\theta}_\sigma \rightarrow v_I.$$

Moreover, the limiting risk admits the representation

$$R_\infty(\theta; \Theta) = \sum_{i=1}^K p_i \|v_i - \theta^*\|^2, \quad p_i := \mathbb{P}(I = i) = \frac{\mu_{d-1}(\mathcal{N}_\Theta(v_i) \cap \mathcal{S}^{d-1})}{\mu_{d-1}(\mathcal{S}^{d-1})}.$$

Remark 2.6. In the diverging-noise regime, estimation over a convex polytope becomes effectively a discrete selection problem among its vertices. By Lemma 2.5, for each vertex v_i of the polytope Θ , the event $\{I = i\}$ occurs precisely when the random direction $U = \frac{Z}{\|Z\|}$ lies in the normal cone $\mathcal{N}_\Theta(v_i)$. Thus, the estimator selects a single vertex v_I , and the risk is the expected squared error incurred by this random vertex choice.

From this perspective, what governs the risk is not only which vertices are close to θ^* , but how often they are selected. Even if a vertex v_i lies close to θ^* in squared distance, its contribution to the risk can increase or decrease depending on whether the probability p_i of selecting it grows or shrinks. This viewpoint clarifies how risk reversal can occur. Consider nested polytopes $\Theta_S \subset \Theta_L$, and suppose for concreteness that

$$\Theta_L = \text{conv}(\Theta_S \cup \{v\})$$

for some additional vertex v . Adding v introduces a new normal cone with positive spherical measure. Since the normal cones partition \mathbb{S}^{d-1} up to a null set, this necessarily redistributes selection probability across vertices: some vertices lose probability mass while others gain it. Risk reversal arises when this redistribution transfers probability mass away from vertices that are far from θ^* toward vertices that are closer to θ^* , thereby reducing risk. Conversely, shrinking the constraint can eliminate or diminish the selection region of a nearby vertex, forcing its probability mass to be reassigned to more distant vertices and increasing risk. \square

We apply the theory of this section to compute the diverging-noise risk expressions for Example 1.1. We begin by establishing the following key lemma, which forms the basis of the subsequent risk computations.

Lemma 2.7. *Fix $c > 0$ and $x \in (0, \frac{1}{c})$. Define $\Theta_x := \text{conv}\{v_1, v_2, v_x\}$, where*

$$v_1 = (0, 0), \quad v_2 = \left(\frac{1}{c}, 1\right), \quad v_x = (x, 1).$$

Then,

$$R_\infty(\theta^*; \Theta_x) = \left(1 + \frac{1}{c^2}\right) \left(\frac{1}{4} + \frac{1}{2\pi} \arctan \frac{1}{c}\right) + (1 + x^2) \left(\frac{1}{4} - \frac{1}{2\pi} \arctan x\right) + o(1).$$

Since in Example 1.1, Θ_L corresponds to Θ_x in Lemma 2.7 with $x = 0$, and Θ_S corresponds to $x = \frac{1}{c}$, the diverging-noise limiting risks follow easily.

Corollary 2.8. *In the setting of Example 1.1, as $\sigma \rightarrow \infty$,*

$$\begin{aligned} R_\sigma(\theta^*; \Theta_S) &= \frac{\alpha_c}{2} + o(1), \\ R_\sigma(\theta^*; \Theta_L) &= \alpha_c \left(\frac{1}{4} + \frac{1}{2\pi} \arctan \frac{1}{c}\right) + \frac{1}{4} + o(1), \end{aligned}$$

where $\alpha_c = 1 + \frac{1}{c^2}$. Consequently, if $0 < c < 1$, $R_\sigma(\theta^*; \Theta_S) > R_\sigma(\theta^*; \Theta_L) + o(1)$.

Remark 2.9 (Risk reversal is not a dimensional phenomenon). Since the running example of this work, Example 1.1, involves constraint sets of different dimensions—namely, $\dim(\Theta_L) = 2$ and $\dim(\Theta_S) = 1$ —one might suspect that the risk reversal arises from this difference in dimension. We show that this is not the case. For any $x \in (0, \frac{1}{c})$ the set Θ_x defined in Lemma 2.7 satisfies $\Theta_x \subset \Theta_L$ and $\dim(\Theta_x) = 2$. By Lemma 2.5

$$R_\infty(\theta^*; \Theta_x) - R_\infty(\theta^*; \Theta_L) = \frac{1+x^2}{2\pi} \left(\frac{\pi}{2} \frac{x^2}{1+x^2} - \arctan x\right) =: \Delta(x).$$

The function $\Delta(x)$ is negative for $x \in (0, 1)$, vanishes at $x = 1$, and is positive for $x > 1$. Consequently, when $c < 1$, there exists an open interval of values $x \in (1, \frac{1}{c})$ for which

$$R_\infty(\theta^*; \Theta_x) > R_\infty(\theta^*; \Theta_L),$$

yielding a continuum of instances of risk reversal among parameter sets of the same dimension. \square

2.2.2 Worst-case risk

In this section, we study worst-case risk reversal and develop the technical tools needed to prove Theorem 1.3. Recall that worst-case risk reversal occurs when two nested constraint sets $\Theta_S \subset \Theta_L$ satisfy

$$\sup_{\theta \in \Theta_S} R_\sigma(\theta; \Theta_S) > \sup_{\theta \in \Theta_L} R_\sigma(\theta; \Theta_L),$$

so that the constrained estimator associated with the smaller feasible set has strictly larger worst-case risk.

Our first step is to strengthen the pointwise diverging-noise convergence of the risk function established in Theorem 2.4. We show that this convergence can be upgraded to a uniform statement over the parameter space.

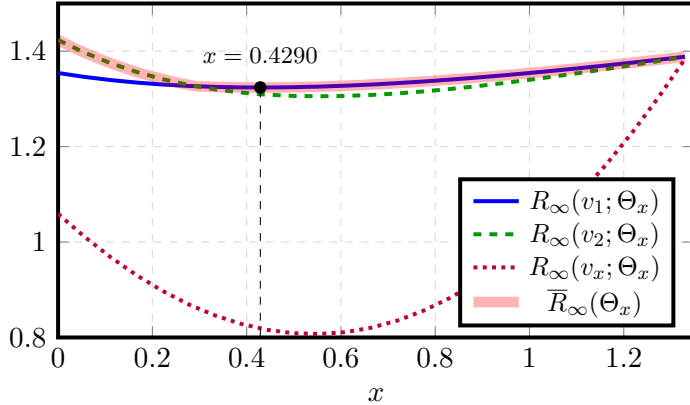


Figure 5 Vertex risks $R_\infty(v_1; \Theta_x)$, $R_\infty(v_2; \Theta_x)$, and $R_\infty(v_x; \Theta_x)$, together with their upper envelope $\bar{R}_\infty(\Theta_x)$, as functions of x for $c = 0.75$. The envelope has a minimum at $x = 0.4290$. Increasing x tightens the constraint. The non-monotonicity of the envelope implies worst-case risk reversal (see Remark 2.13).

Lemma 2.10. Let $\Theta \subset \mathbb{R}^d$ be nonempty, compact, and convex. Then as $\sigma \rightarrow \infty$,

$$\sup_{\theta \in \Theta} R_\sigma(\theta; \Theta) \rightarrow \sup_{\theta \in \Theta} R_\infty(\theta; \Theta).$$

This uniform convergence result plays a central role in our analysis. It allows us to infer worst-case properties of the finite-noise risk R_σ from the corresponding properties of the limiting risk R_∞ . In particular, a strict separation between worst-case limiting risks implies the same ordering for all sufficiently large but finite noise levels.

Theorem 2.11. Let $\Theta_S \subset \Theta_L$ be nonempty, compact, and convex. Suppose that

$$\sup_{\theta \in \Theta_S} R_\infty(\theta; \Theta_S) > \sup_{\theta \in \Theta_L} R_\infty(\theta; \Theta_L).$$

Then there exists $\sigma_0 < \infty$ such that for all $\sigma \geq \sigma_0$,

$$\sup_{\theta \in \Theta_S} R_\sigma(\theta; \Theta_S) > \sup_{\theta \in \Theta_L} R_\sigma(\theta; \Theta_L).$$

By Theorem 2.11, to establish worst-case risk reversal at a finite noise level, it suffices to identify nested constraint sets $\Theta_S \subset \Theta_L$ whose limiting risks exhibit worst-case reversal. This task is substantially simplified by the geometric structure of convex polytopes. In particular, Lemma 2.5 shows that the worst-case limiting risk over a polytope is attained at one of its vertices, allowing for an explicit and tractable verification of the phenomenon. We now demonstrate this construction.

Lemma 2.12. Fix $c = 0.75$, $a = 0.5$, and $b = 1.3$. Define

$$v_1 = (0, 0), \quad v_2 = \left(\frac{1}{c}, 1\right), \quad v_a = (a, 1), \quad v_b = (b, 1).$$

Let

$$\Theta_S := \text{conv}\{v_1, v_2, v_b\}, \quad \Theta_L := \text{conv}\{v_1, v_2, v_a\}.$$

Then $\Theta_S \subset \Theta_L$ and

$$\sup_{\theta \in \Theta_S} R_\infty(\theta; \Theta_S) > \sup_{\theta \in \Theta_L} R_\infty(\theta; \Theta_L).$$

Remark 2.13. Figure 5 provides geometric intuition for the construction in Lemma 2.12. For each $x \in (0, 1/c)$, the large-noise risk $R_\infty(\theta; \Theta_x)$ is a convex quadratic function of θ , and hence its maximum over the compact convex set Θ_x is attained at an extreme point. As a result, the worst-case risk over Θ_x reduces to the maximum of the risks evaluated at the three vertices v_1 , v_2 , and v_x .

The figure plots these three vertex risks, as well as their upper envelope

$$\bar{R}_\infty(\Theta_x) := \max\{R_\infty(v_1; \Theta_x), R_\infty(v_2; \Theta_x), R_\infty(v_x; \Theta_x)\},$$

as functions of x for $c = 0.75$. Increasing x tightens the constraint, since $\Theta_{x_2} \subset \Theta_{x_1}$ whenever $x_2 > x_1$. If tightening the constraint could only improve performance, the envelope $\bar{R}_\infty(\Theta_x)$ would be non-increasing in x . Instead, the plot exhibits a non-monotone behavior: the envelope initially decreases, but eventually increases as x grows. This behavior underlies the strict worst-case risk reversal established in Lemma 2.12. \square

3 Proofs

In this section, we provide the proofs and supporting results omitted from sections 1.2, 2.1 and 2.2.2.

3.1 Proofs of results in Section 1.2

Our risk expressions involve *Owen's T-function* [Owe80], defined for $h, a \in \mathbb{R}$ by

$$T(h, a) := \phi(h) \int_0^a \frac{\phi(hz)}{1+z^2} dz,$$

where ϕ denotes the probability density function of a unit Gaussian. We also introduce the notation Φ to denote the cumulative distribution function of a unit Gaussian. For completeness, in Appendix A we recall some basic properties of Owen's T-function that we make use of in the following risk analyses.

3.1.1 Risk analysis of $\hat{\theta}_L$

The LSE $\hat{\theta}_L$ exhibits piecewise behavior depending on the location of $y \in \mathbb{R}^2$. Define $s_c(y) := \frac{y_1 + cy_2}{1+c^2}$. We partition \mathbb{R}^2 into the following regions (see Figure 1), on each of which $\hat{\theta}_L$ admits a simple closed-form expression.

Region	Definition (y_1, y_2)	$\hat{\theta}_L(y)$	Face of Θ_L
Θ_L	$0 \leq y_1 \leq \frac{1}{c}$, $0 \leq y_2 \leq 1$, $y_2 \geq cy_1$	(y_1, y_2)	Interior
A_1	$y_1 \leq -cy_2$, $y_2 \leq 0$	$(0, 0)$	Vertex v_1
A_2	$y_1 \geq \frac{1}{c}$, $y_2 \geq 1 - \frac{1}{c}(y_1 - \frac{1}{c})$	$(\frac{1}{c}, 1)$	Vertex v_2
A_3	$y_1 \leq 0$, $y_2 \geq 1$	$(0, 1)$	Vertex v_3
A_{12}	$y_2 \leq cy_1$, $0 \leq s_c(y) \leq \frac{1}{c}$	$(s_c(y), cs_c(y))$	Edge $[v_1, v_2]$
A_{13}	$y_1 \leq 0$, $0 \leq y_2 \leq 1$	$(0, y_2)$	Edge $[v_1, v_3]$
A_{23}	$0 \leq y_1 \leq \frac{1}{c}$, $y_2 \geq 1$	$(y_1, 1)$	Edge $[v_2, v_3]$

Theorem 3.1. *In the setting of Example 1.1,*

$$\begin{aligned}
R_\sigma(\theta^*; \Theta_L) &= -\sigma\phi\left(\frac{1}{\sigma}\right)\Phi\left(\frac{1}{c\sigma}\right) + \sigma^2\left[\frac{1}{2}\left(\Phi\left(\frac{1}{\sigma}\right) - \frac{1}{2}\right) - 2T\left(\frac{1}{\sigma}, \frac{1}{c}\right) + \frac{1}{\pi}\arctan\frac{1}{c}\right] \\
&\quad + \Phi\left(-\frac{1}{\sigma}\right)\left[\sigma^2\left(\Phi\left(\frac{1}{c\sigma}\right) - \frac{1}{c\sigma}\phi\left(\frac{1}{c\sigma}\right) - \frac{1}{2}\right) + \Phi\left(\frac{1}{c\sigma}\right)\right] \\
&\quad + \frac{\sigma^2}{2}\left(\Phi\left(\frac{\sqrt{\alpha_c}}{\sigma}\right) - \frac{\sqrt{\alpha_c}}{\sigma}\phi\left(\frac{\sqrt{\alpha_c}}{\sigma}\right) - \frac{1}{2}\right) \\
&\quad + \alpha_c\left[\Phi\left(-\frac{1}{c\sigma}\right)\Phi\left(-\frac{\sqrt{\alpha_c}}{\sigma}\right) + T\left(\frac{1}{c\sigma}, \sqrt{c^2+1}\right) + T\left(\frac{\sqrt{\alpha_c}}{\sigma}, \frac{1}{\sqrt{c^2+1}}\right) - T\left(\frac{1}{c\sigma}, c\right)\right]
\end{aligned}$$

where $\alpha_c = 1 + \frac{1}{c^2}$.

Proof. We compute the contribution to the risk from each of the regions $\Theta_L, A_1, A_2, A_3, A_{12}, A_{13}$ and A_{23} defined above. Throughout, we write $r_\sigma(\theta^*; A)$ to denote the risk restricted to a region A , namely

$$r_\sigma(\theta^*; A) := \mathbb{E}[\|\hat{\theta}_L - \theta^*\|^2 \mathbf{1}\{Y \in A\}].$$

Risk on Θ_L : $\hat{\theta}_L = (y_1, y_2)$, and so $\|\hat{\theta}_L - \theta^*\|^2 = y_1^2 + y_2^2$. We have

$$r_\sigma(\theta^*; \Theta_L) = \int_{y_2=0}^1 \int_{y_1=0}^{\frac{y_2}{c}} (y_1^2 + y_2^2) \frac{\phi(\frac{y_1}{\sigma})}{\sigma} \frac{\phi(\frac{y_2}{\sigma})}{\sigma} dy_1 dy_2 =: T_1 + T_2.$$

For T_1 , we have

$$\begin{aligned}
T_1 &= \sigma^2 \int_{y_2=0}^1 \frac{\phi(\frac{y_2}{\sigma})}{\sigma} \left(\int_0^{\frac{y_2}{c\sigma}} z^2 \phi(z) dz \right) dy_2 \\
&= \sigma^2 \int_0^{\frac{1}{\sigma}} \phi(z) \left(\Phi\left(\frac{z}{c}\right) - \frac{z}{c}\phi\left(\frac{z}{c}\right) - \frac{1}{2} \right) dz \\
&= \sigma^2 \left(\frac{1}{2\pi} \arctan \frac{1}{c} - T\left(\frac{1}{\sigma}, \frac{1}{c}\right) - \frac{\phi(0)\phi(\frac{\sqrt{\alpha_c}}{\sigma})}{c\alpha_c} \left(\phi(0) - \phi\left(\frac{\sqrt{\alpha_c}}{\sigma}\right) \right) \right),
\end{aligned}$$

where the last line holds by Proposition A.1. For T_2 ,

$$\begin{aligned}
T_2 &= \sigma^2 \int_0^{\frac{1}{\sigma}} z^2 \phi(z) \left(\Phi\left(\frac{z}{c}\right) - \frac{1}{2} \right) dz \\
&= \sigma^2 \left(\frac{1}{\sigma} \phi\left(\frac{1}{\sigma}\right) \left(\frac{1}{2} - \Phi\left(\frac{1}{c\sigma}\right) \right) - T\left(\frac{1}{\sigma}, \frac{1}{c}\right) - \frac{\phi(0)\phi(\frac{\sqrt{\alpha_c}}{\sigma})}{c\alpha_c} + \frac{1}{2\pi} \arctan \frac{1}{c} + \frac{(\phi(0))^2}{c\alpha_c} \right).
\end{aligned}$$

Putting it together, we have

$$r_\sigma(\theta^*; \Theta_L) = \sigma^2 \left(\frac{1}{\sigma} \phi\left(\frac{1}{\sigma}\right) \left(\frac{1}{2} - \Phi\left(\frac{1}{c\sigma}\right) \right) - 2T\left(\frac{1}{\sigma}, \frac{1}{c}\right) + \frac{1}{\pi} \arctan \frac{1}{c} \right).$$

Risk on A_1 : $\hat{\theta}_L = (0, 0)$, so $r_\sigma(\theta^*; A_1) = 0$.

Risk on A_2 : $\hat{\theta}_L = (\frac{1}{c}, 1)$. We have

$$r_\sigma(\theta^*; A_2) = \alpha_c \left(\int_{y_2=1}^{\infty} \int_{y_1=\frac{1}{c}}^{\infty} + \int_{y_1=\frac{1}{c}}^{\infty} \int_{y_2=-\frac{y_1}{c}+\alpha_c}^1 \right) \frac{\phi(\frac{y_1}{\sigma})}{\sigma} \frac{\phi(\frac{y_2}{\sigma})}{\sigma} dy_1 dy_2 =: T_1 + T_2.$$

It is straight forward to show

$$T_1 = \alpha_c \Phi\left(-\frac{1}{c\sigma}\right) \Phi\left(-\frac{1}{\sigma}\right).$$

For T_2 , direct calculation gives

$$T_2 = \alpha_c \int_{\frac{1}{c\sigma}}^{\infty} \phi(z) \left[\Phi\left(\frac{1}{\sigma}\right) - \Phi\left(\frac{\alpha_c}{\sigma} - \frac{z}{c}\right) \right] = \alpha_c \left(\Phi\left(-\frac{1}{c\sigma}\right) \Phi\left(\frac{1}{\sigma}\right) - T_{21} \right).$$

By Proposition A.1,

$$T_{21} = \Phi\left(\frac{\sqrt{\alpha_c}}{\sigma}\right) \Phi\left(-\frac{1}{c\sigma}\right) - T\left(\frac{1}{c\sigma}, c\sqrt{\alpha_c}\right) - T\left(\frac{\sqrt{\alpha_c}}{\sigma}, \frac{1}{c\sqrt{\alpha_c}}\right) + T\left(\frac{1}{c\sigma}, c\right).$$

Putting it together and simplifying gives

$$r_\sigma(\theta^*; A_2) = \alpha_c \left(\Phi\left(-\frac{\sqrt{\alpha_c}}{\sigma}\right) \Phi\left(-\frac{1}{c\sigma}\right) + T\left(\frac{1}{c\sigma}, c\sqrt{\alpha_c}\right) + T\left(\frac{\sqrt{\alpha_c}}{\sigma}, \frac{1}{c\sqrt{\alpha_c}}\right) - T\left(\frac{1}{c\sigma}, c\right) \right).$$

Risk on A_3 : $\hat{\theta}_L = (0, 1)$. We have

$$r_\sigma(\theta^*; A_3) = \int_{y_2=1}^{\infty} \int_{y_1=-\infty}^0 \frac{\phi(\frac{y_1}{\sigma})}{\sigma} \frac{\phi(\frac{y_2}{\sigma})}{\sigma} dy_1 dy_2 = \frac{1}{2} \Phi\left(-\frac{1}{\sigma}\right).$$

Risk on A_{12} : $\hat{\theta}_L = (s_c(y), cs_c(y))$ where $s_c(y) = \frac{y_1+cy_2}{1+c^2}$. Directly computing integrals in this case is particularly tedious and so we opt for a statistical approach instead. Note that

$$\|\hat{\theta}_L\|^2 = (1+c^2)(s_c(y))^2 = \frac{(y_1+cy_2)^2}{1+c^2}.$$

Define

$$X := \frac{Z_1 + cZ_2}{\sqrt{1+c^2}}, \quad W := \frac{Z_2 - cZ_1}{\sqrt{1+c^2}}.$$

Note that $\|\hat{\theta}_L\|^2 = \sigma^2 X^2$. We now rewrite the event A_{12} in terms of X, W . First,

$$y_2 \leq cy_1 \iff Z_2 \leq cZ_1 \iff W \leq 0,$$

and second

$$0 \leq s_c(y) \leq \frac{1}{c} \iff 0 \leq X \leq \frac{\sqrt{\alpha_c}}{\sigma}.$$

Hence, $A_{12} = \{W \leq 0\} \cap \{0 \leq X \leq \frac{\sqrt{\alpha_c}}{\sigma}\}$. Importantly, since $Z_1, Z_2 \stackrel{\text{i.i.d.}}{\sim} N(0, 1)$, it follows that $X, W \stackrel{\text{i.i.d.}}{\sim} N(0, 1)$. Therefore,

$$\begin{aligned} r_\sigma(\theta^*; A_{12}) &= \mathbb{E}[\|\hat{\theta}_L\|^2 \mathbf{1}\{A_{12}\}] = \sigma^2 \mathbb{E}\left[X^2 \mathbf{1}\{W \leq 0\} \mathbf{1}\left\{0 \leq X \leq \frac{\sqrt{\alpha_c}}{\sigma}\right\}\right] \\ &= \sigma^2 \mathbb{E}\left[X^2 \mathbf{1}\left\{0 \leq X \leq \frac{\sqrt{\alpha_c}}{\sigma}\right\}\right] \mathbb{P}(W \leq 0) = \frac{\sigma^2}{2} \int_0^{\frac{\sqrt{\alpha_c}}{\sigma}} x^2 \phi(x) dx \\ &= \frac{\sigma^2}{2} \left(\Phi\left(\frac{\sqrt{\alpha_c}}{\sigma}\right) - \frac{1}{2} - \frac{\sqrt{\alpha_c}}{\sigma} \phi\left(\frac{\sqrt{\alpha_c}}{\sigma}\right) \right), \end{aligned}$$

where the third equality follows by the independence of X, W .

Risk on A_{13} : $\hat{\theta}_L = (0, y_2)$. We have

$$r_\sigma(\theta^*; A_{13}) = \int_{y_2=0}^1 \int_{y_1=-\infty}^0 y_2^2 \frac{\phi(\frac{y_1}{\sigma})}{\sigma} \frac{\phi(\frac{y_2}{\sigma})}{\sigma} dy_1 dy_2 = \frac{\sigma^2}{2} \int_0^{\frac{1}{\sigma}} z^2 \phi(z) dz = \frac{\sigma^2}{2} \left(\Phi\left(\frac{1}{\sigma}\right) - \frac{1}{\sigma} \phi\left(\frac{1}{\sigma}\right) - \frac{1}{2} \right).$$

Risk on A_{23} : $\hat{\theta}_L = (y_1, 1)$. We have

$$\begin{aligned} r_\sigma(\theta^*; A_{23}) &= \int_{y_2=1}^{\infty} \int_{y_1=0}^{\frac{1}{c}} (1 + y_1^2) \frac{\phi(\frac{y_1}{\sigma})}{\sigma} \frac{\phi(\frac{y_2}{\sigma})}{\sigma} dy_1 dy_2 = \Phi\left(\frac{-1}{\sigma}\right) \int_0^{\frac{1}{c\sigma}} (1 + \sigma^2 z^2) \phi(z) dz \\ &= \Phi\left(\frac{-1}{\sigma}\right) \left[(1 + \sigma^2) \left(\Phi\left(\frac{1}{c\sigma}\right) - \frac{1}{2} \right) - \frac{\sigma}{c} \phi\left(\frac{1}{c\sigma}\right) \right]. \end{aligned}$$

□

3.1.2 Risk analysis of $\hat{\theta}_S$

Theorem 3.2. *In the setting of Example 1.1,*

$$R_\sigma(\theta^*; \Theta_S) = \sigma^2 \left(\Phi\left(\frac{\sqrt{\alpha_c}}{\sigma}\right) - \frac{1}{2} - \frac{\sqrt{\alpha_c}}{\sigma} \phi\left(\frac{\sqrt{\alpha_c}}{\sigma}\right) \right) + \alpha_c \Phi\left(-\frac{\sqrt{\alpha_c}}{\sigma}\right),$$

where $\alpha_c = 1 + \frac{1}{c^2}$.

Proof. We prove a more general result by letting θ^* be an arbitrary element of Θ_S and then specialize to the $\theta^* = v_1$ case. Note that we can write

$$\Theta_S = \{tv_2 : t \in [0, 1]\},$$

and so $\theta^* = t^* v_2$ for some $t^* \in [0, 1]$. Since Θ_S is simply a (truncated) line segment, the orthogonal projection onto Θ_S takes a particular simple form. Specifically, we have $\hat{\theta}_S = \hat{t} v_2$, where

$$\hat{t} := \text{clip}\left(\frac{\langle Y, v_2 \rangle}{\|v_2\|^2}, 0, 1\right), \quad \text{clip}(x, 0, 1) := \min(1, \max(0, x)).$$

Recall $\|v_2\|^2 = 1 + \frac{1}{c^2} = \alpha_c$. Now, we have

$$Y = \theta^* + \sigma Z = t^* v_2 + \sigma Z$$

which implies

$$\frac{\langle Y, v_2 \rangle}{\alpha_c} = t^* + \sigma \frac{\langle Z, v_2 \rangle}{\alpha_c} \stackrel{d}{=} t^* + \frac{\sigma}{\sqrt{\alpha_c}} g, \quad g \sim N(0, 1),$$

where we have used the fact that $\langle Z, v_2 \rangle \sim N(0, \alpha_c) \stackrel{d}{=} \sqrt{\alpha_c} g$. Using this, we define the un-clipped estimator

$$\tilde{t} := \frac{\langle Y, v_2 \rangle}{\alpha_c} = t^* + \frac{\sigma}{\sqrt{\alpha_c}} g,$$

and so $\hat{t} = \text{clip}(\tilde{t}, 0, 1)$. The risk is then

$$R_\sigma(\theta^*; \Theta_S) = \mathbb{E}\|\hat{t}v_2 - t^*v_2\|^2 = \alpha_c \mathbb{E}(\hat{t} - t^*)^2.$$

Note that the event $\{\tilde{t} \in [0, 1]\}$ is equivalent to the event $\{g \in [-\frac{\sqrt{\alpha_c}t^*}{\sigma}, \frac{\sqrt{\alpha_c}(1-t^*)}{\sigma}]\}$. To ease notation, for the remainder of the proof let: $a := -\frac{\sqrt{\alpha_c}t^*}{\sigma}$ and $b := \frac{\sqrt{\alpha_c}(1-t^*)}{\sigma}$. Direct calculation then yields

$$\begin{aligned} \mathbb{E}(\hat{t} - t^*)^2 &= \mathbb{E}(\hat{t} - t^*)^2 \mathbf{1}\{g \leq a\} + \mathbb{E}(\hat{t} - t^*)^2 \mathbf{1}\{g \in [a, b]\} + \mathbb{E}(\hat{t} - t^*)^2 \mathbf{1}\{g \geq b\} \\ &= (t^*)^2 \mathbb{P}(g \leq a) + \mathbb{E}(\tilde{t} - t^*)^2 \mathbf{1}\{g \in [a, b]\} + (1 - t^*)^2 \mathbb{P}(g \geq b) \\ &= (t^*)^2 \Phi(a) + \frac{\sigma^2}{\alpha_c} \mathbb{E}[g^2 \mathbf{1}\{g \in [a, b]\}] + (1 - t^*)^2 \Phi(-b) \\ &= (t^*)^2 \Phi(a) + \frac{\sigma^2}{\alpha_c} (\Phi(b) - \Phi(a) - b\phi(b) + a\phi(a)) + (1 - t^*)^2 \Phi(-b), \end{aligned}$$

where we have used the fact that

$$\mathbb{E}[g^2 \mathbf{1}\{g \in [a, b]\}] = \int_a^b z^2 \phi(z) dz = \Phi(b) - \Phi(a) - b\phi(b) + a\phi(a).$$

The result follows by taking $t^* = 0$. \square

Proof of Theorem 1.2. The explicit expressions for the risk are given in Theorems 3.1 and 3.2. The vanishing-noise expansions in (2) follow by Corollary 2.3. Since $c > 0$ implies $\arctan \frac{1}{c} \in (0, \frac{\pi}{2})$, the leading constant is strictly negative, and therefore $R_\sigma(\theta^*; \Theta_S) - R_\sigma(\theta^*; \Theta_L) < 0$ for all sufficiently small σ . The diverging-noise expansions (3) follow by Corollary 2.8. Writing the leading term as

$$g(c) := \frac{1}{4c^2} - \frac{1+c^2}{2\pi c^2} \arctan \frac{1}{c} = \frac{1}{4c^2} \left(1 - \frac{2}{\pi} (1+c^2) \arctan \frac{1}{c} \right),$$

we see that its sign is determined by the function $h(c) := (1+c^2) \arctan \frac{1}{c}$. Differentiating shows that h is strictly decreasing on $(0, \infty)$, with $h(1) = \frac{\pi}{2}$. Consequently, $h(c) > \frac{\pi}{2}$ for $0 < c < 1$, $h(c) = \frac{\pi}{2}$ for $c = 1$, and $h(c) < \frac{\pi}{2}$ for $c > 1$. This yields

$$g(c) \begin{cases} > 0, & 0 < c < 1, \\ = 0, & c = 1, \\ < 0, & c > 1, \end{cases}$$

and the stated ordering for sufficiently large σ follows from (3). \square

3.2 Proofs of results in Section 2.1

We first present a proof of the vanishing-noise risk behavior of the LSE. While the statement recovers [OH16, Theorem 3.1], our argument is based on a distinct proof strategy grounded in the theory of differentiability of metric projections [Zar71].

Proposition 3.3. *Let $\Theta \subset \mathbb{R}^d$ be a compact and convex set with nonempty interior. Fix $\theta^* \in \Theta$ and for $\sigma > 0$, define*

$$\hat{\theta}_\sigma := \Pi_\Theta(\theta^* + \sigma Z), \quad Z \sim N(0, I_d).$$

(i) **Boundary case.** *If $\theta^* \in \partial\Theta$, then as $\sigma \rightarrow 0^+$,*

$$\frac{\hat{\theta}_\sigma - \theta^*}{\sigma} \xrightarrow{L^2} \Pi_{T_\Theta(\theta^*)}(Z), \quad (6)$$

and consequently

$$\mathbb{E}\|\hat{\theta}_\sigma - \theta^*\|^2 = \sigma^2 \delta(T_\Theta(\theta^*)) + o(\sigma^2). \quad (7)$$

(ii) **Interior case.** *If $\theta^* \in \text{int}(\Theta)$, then as $\sigma \rightarrow 0^+$,*

$$\frac{\hat{\theta}_\sigma - \theta^*}{\sigma} \xrightarrow{L^2} Z. \quad (8)$$

Moreover, for every integer $m \geq 1$,

$$\mathbb{E}\|\hat{\theta}_\sigma - \theta^*\|^2 = \sigma^2 d + o(\sigma^m). \quad (9)$$

Proof. For $\sigma > 0$, define the scaled mapping

$$G_\sigma(u) := \frac{\Pi_\Theta(\theta^* + \sigma u) - \theta^*}{\sigma}, \quad u \in \mathbb{R}^d,$$

so that $(\hat{\theta}_\sigma - \theta^*)/\sigma = G_\sigma(Z)$. Since $\theta^* \in \Theta$, by properties of the projection operator

$$\|\Pi_\Theta(\theta^* + \sigma u) - (\theta^* + \sigma u)\| \leq \|\theta^* - (\theta^* + \sigma u)\| = \sigma\|u\|.$$

Therefore,

$$\|\Pi_\Theta(\theta^* + \sigma u) - \theta^*\| \leq \|\Pi_\Theta(\theta^* + \sigma u) - (\theta^* + \sigma u)\| + \|(\theta^* + \sigma u) - \theta^*\| \leq 2\sigma\|u\|,$$

and hence for all $\sigma > 0$ and $u \in \mathbb{R}^d$,

$$\|G_\sigma(u)\| \leq 2\|u\|. \quad (10)$$

Also, for any closed convex cone C , $\|\Pi_C(u)\| \leq \|u\|$.

Boundary case. Assume $\theta^* \in \partial\Theta$. Since Θ is compact, convex, and has nonempty interior, the projection Π_Θ is one-sided directionally differentiable at every boundary point [Zar71, Sha16]. More precisely, for each $u \in \mathbb{R}^d$,

$$\lim_{t \rightarrow 0^+} \frac{\Pi_\Theta(\theta^* + tu) - \theta^*}{t} = \Pi_{S_\Theta(\theta^*)}(u),$$

where $S_\Theta(\theta^*)$ is the support cone of Θ at θ^* . For a compact, convex set, the support cone coincides with the tangent cone, i.e. $S_\Theta(\theta^*) = T_\Theta(\theta^*)$. Taking $t = \sigma$ shows that $G_\sigma(u) \rightarrow \Pi_{T_\Theta(\theta^*)}(u)$ for each fixed u . Evaluating at Z , we obtain almost sure convergence $G_\sigma(Z) \rightarrow \Pi_{T_\Theta(\theta^*)}(Z)$. Moreover, by (10),

$$\|G_\sigma(Z) - \Pi_{T_\Theta(\theta^*)}(Z)\|^2 \leq 2\|G_\sigma(Z)\|^2 + 2\|\Pi_{T_\Theta(\theta^*)}(Z)\|^2 \leq 10\|Z\|^2,$$

and since $\mathbb{E}\|Z\|^2 < \infty$, dominated convergence yields

$$\mathbb{E}\|G_\sigma(Z) - \Pi_{T_\Theta(\theta^*)}(Z)\|^2 \rightarrow 0,$$

which proves (6). Then (7) follows from

$$\mathbb{E}\|\hat{\theta}_\sigma - \theta^*\|^2 = \sigma^2 \mathbb{E}\|G_\sigma(Z)\|^2 = \sigma^2(\mathbb{E}\|\Pi_{T_\Theta(\theta^*)}(Z)\|^2 + o(1)).$$

Interior case. Assume $\theta^* \in \text{int}(\Theta)$ and let $r := \inf_{\theta \in \partial\Theta} \|\theta^* - \theta\| > 0$. Then $B(\theta^*, r) \subset \Theta$. Define $A_\sigma := \{\|Z\| \leq r/\sigma\}$. On A_σ , $\theta^* + \sigma Z \in \Theta$ and hence $G_\sigma(Z) = Z$. Therefore $G_\sigma(Z) \rightarrow Z$ almost surely. To obtain L^2 convergence, note that

$$\mathbb{E}\|G_\sigma(Z) - Z\|^2 = \mathbb{E}[\|G_\sigma(Z) - Z\|^2 \mathbf{1}_{A_\sigma^c}] \leq 10\mathbb{E}[\|Z\|^2 \mathbf{1}_{A_\sigma^c}],$$

and dominated convergence implies (8). Finally, since Π_Θ is a projection onto a closed, convex set, it is 1-Lipschitz and writing $\Pi_\Theta(\theta^*) = \theta^*$, we have

$$\|\hat{\theta}_\sigma - \theta^*\| = \|\Pi_\Theta(\theta^* + \sigma Z) - \Pi_\Theta(\theta^*)\| \leq \sigma\|Z\|.$$

Thus

$$0 \leq \sigma^2 d - \mathbb{E}\|\hat{\theta}_\sigma - \theta^*\|^2 \leq \sigma^2 \mathbb{E}[\|Z\|^2 \mathbf{1}_{\{\|Z\| > r/\sigma\}}].$$

Standard χ^2 tail bounds imply that the right-hand side is $o(\sigma^m)$ for every $m \geq 1$, which proves (9). \square

Proof of Theorem 2.1. By [ALMT14, Proposition 3.1], the statistical dimension is monotone with respect to inclusion: for closed convex cones $K_1, K_2 \subset \mathbb{R}^d$, the inclusion $K_1 \subset K_2$ implies

$$\delta(K_1) \leq \delta(K_2).$$

Applying the asymptotic risk expansion of [OH16, Theorem 3.1] and invoking the monotonicity of the statistical dimension completes the proof. \square

Proof of Corollary 2.3. We proceed by computing the statistical dimension of the tangent cone of Θ_S and Θ_L at θ^* . The result then follows by applying [OH16, Theorem 3.1]. Since Θ_S is the line segment joining v_1 and v_2 , the feasible directions at the endpoint v_1 are exactly the nonnegative multiples of v_2 , hence

$$T_{\Theta_S}(\theta^*) = \{tv_2 : t \geq 0\}.$$

Similarly, Θ_L is the triangle with vertex $\theta^* = v_1$ and edges along v_2 and v_3 , so the feasible directions at v_1 form the conic hull of $\{v_2, v_3\}$:

$$T_{\Theta_L}(\theta^*) = \{sv_2 + tv_3 : s, t \geq 0\}.$$

We recall the following definitions [ALMT14, Section 5.1]. Let $C \subset \mathbb{R}^2$ be a polyhedral cone. Its (conic) intrinsic volumes are the numbers $\Gamma_k(C) \in [0, 1]$, $k = 0, 1, 2$, defined by

$$\Gamma_k(C) := \mathbb{P}(\Pi_C(Z) \text{ lies in the relative interior of a } k\text{-dimensional face of } C), \quad Z \sim N(0, I_2).$$

These quantities satisfy $\sum_{k=0}^2 \Gamma_k(C) = 1$, and the statistical dimension admits the representation $\delta(C) = \sum_{k=0}^2 k\Gamma_k(C)$. We apply this result to $T_{\Theta_S}(\theta^*)$ and $T_{\Theta_L}(\theta^*)$ as they are both polyhedral cones.

- $T_{\Theta_S}(\theta^*)$. This cone has exactly two faces: the vertex v_1 (dimension 0) and the ray itself (dimension 1). Hence $\Gamma_2(T_{\Theta_S}(\theta^*)) = 0$. Moreover, by symmetry of the standard Gaussian, the scalar projection of Z onto the direction v_2 is nonnegative with probability $\frac{1}{2}$, and negative with probability $\frac{1}{2}$. When it is negative, the closest point in $T_{\Theta_S}(\theta^*)$ is the origin. Therefore

$$\Gamma_0(T_{\Theta_S}(\theta^*)) = \mathbb{P}(\Pi_{T_{\Theta_S}(\theta^*)}(Z) = 0) = \frac{1}{2}, \quad \Gamma_1(T_{\Theta_S}(\theta^*)) = 1 - \Gamma_0(T_{\Theta_S}(\theta^*)) - \Gamma_2(T_{\Theta_S}(\theta^*)) = \frac{1}{2}.$$

Therefore

$$\delta(T_{\Theta_S}(\theta^*)) = 0 \cdot \Gamma_0(T_{\Theta_S}(\theta^*)) + 1 \cdot \Gamma_1(T_{\Theta_S}(\theta^*)) + 2 \cdot \Gamma_2(T_{\Theta_S}(\theta^*)) = \frac{1}{2}.$$

- $T_{\Theta_L}(\theta^*)$. Let $\theta = \arctan \frac{1}{c} \in (0, \pi)$ denote the angle between the rays spanned by v_2 and v_3 . Because Z is rotationally invariant, the probability that Z falls into the wedge $T_{\Theta_L}(\theta^*)$ depends only on θ , and equals $\frac{\theta}{2\pi}$. Whenever $Z \in \text{int}(T_{\Theta_L}(\theta^*))$, we have $\Pi_{T_{\Theta_L}(\theta^*)}(Z) = Z$, so the projection lies in the relative interior of the unique 2-dimensional face. Hence

$$\Gamma_2(T_{\Theta_L}(\theta^*)) = \mathbb{P}(Z \in T_{\Theta_L}(\theta^*)) = \frac{\theta}{2\pi}.$$

By the same argument applied to the polar cone $T_{\Theta_L}(\theta^*)^\circ$, whose opening angle is $\pi - \theta$,

$$\Gamma_0(T_{\Theta_L}(\theta^*)) = \mathbb{P}(\Pi_{T_{\Theta_L}(\theta^*)}(Z) = 0) = \mathbb{P}(Z \in T_{\Theta_L}(\theta^*)^\circ) = \frac{\pi - \theta}{2\pi}.$$

Thus

$$\Gamma_1(T_{\Theta_L}(\theta^*)) = 1 - \Gamma_0(T_{\Theta_L}(\theta^*)) - \Gamma_2(T_{\Theta_L}(\theta^*)) = \frac{1}{2}.$$

It follows that

$$\delta(T_{\Theta_L}(\theta^*)) = \Gamma_1(T_{\Theta_L}(\theta^*)) + 2\Gamma_2(T_{\Theta_L}(\theta^*)) = \frac{1}{2} + \frac{\theta}{\pi} = \frac{1}{2} + \frac{1}{\pi} \arctan \frac{1}{c}.$$

Importantly,

$$\delta(T_{\Theta_S}(\theta^*)) = \frac{1}{2} \quad \text{and} \quad \delta(T_{\Theta_L}(\theta^*)) \in \left(\frac{1}{2}, 1\right),$$

and so $\delta(T_{\Theta_S}(\theta^*)) - \delta(T_{\Theta_L}(\theta^*)) < 0$ for any $c > 0$. \square

3.3 Proofs of results in Section 2.2

Proof of Theorem 2.4. Define, for $\sigma > 0$ and $\theta \in \Theta$

$$F_\sigma(\theta) := \langle \theta, U \rangle - \frac{1}{2\sigma \|Z\|} \|\theta - \theta^*\|^2, \quad F_\infty(\theta) := \langle \theta, U \rangle,$$

on the event $\{Z \neq 0\}$, which has probability one. We first show that $\hat{\theta}_\sigma$ is the unique maximizer of F_σ over Θ . By definition,

$$\hat{\theta}_\sigma = \arg \min_{\theta \in \Theta} \|\theta - (\theta^* + \sigma Z)\|^2.$$

Expanding the square and discarding terms independent of θ yields

$$\hat{\theta}_\sigma = \arg \min_{\theta \in \Theta} \left\{ \|\theta - \theta^*\|^2 - 2\sigma \langle \theta, Z \rangle \right\}.$$

Writing $Z = \|Z\|U$ and multiplying by $-\frac{1}{2\sigma\|Z\|}$ gives

$$\hat{\theta}_\sigma = \arg \max_{\theta \in \Theta} \left\{ \langle \theta, U \rangle - \frac{1}{2\sigma\|Z\|} \|\theta - \theta^*\|^2 \right\} = \arg \max_{\theta \in \Theta} F_\sigma(\theta).$$

Since F_σ is strictly concave on \mathbb{R}^d , the maximizer over the convex set Θ is unique.

Next, since Θ is bounded, $F_\sigma \rightarrow F_\infty$ uniformly on Θ almost surely. Indeed, letting $D := \sup_{\theta \in \Theta} \|\theta - \theta^*\| < \infty$, we have

$$\sup_{\theta \in \Theta} |F_\sigma(\theta) - F_\infty(\theta)| = \sup_{\theta \in \Theta} \frac{1}{2\sigma\|Z\|} \|\theta - \theta^*\|^2 \leq \frac{D^2}{2\sigma\|Z\|} \rightarrow 0 \quad \text{a.s.}$$

We now show that every limit point of $\hat{\theta}_\sigma$ lies in $F_\Theta(U)$. Let $\sigma_n \rightarrow \infty$ and suppose $\hat{\theta}_{\sigma_n} \rightarrow \bar{\theta}$. Fix $\varepsilon > 0$ and choose n_0 such that $\sup_{\theta \in \Theta} |F_{\sigma_n}(\theta) - F_\infty(\theta)| \leq \varepsilon$ for all $n \geq n_0$. Then, for $n \geq n_0$,

$$F_\infty(\hat{\theta}_{\sigma_n}) \geq F_{\sigma_n}(\hat{\theta}_{\sigma_n}) - \varepsilon = \sup_{\theta \in \Theta} F_{\sigma_n}(\theta) - \varepsilon \geq \sup_{\theta \in \Theta} F_\infty(\theta) - 2\varepsilon.$$

Letting $n \rightarrow \infty$ and using continuity of $F_\infty(\theta) = \langle \theta, U \rangle$ yields

$$F_\infty(\bar{\theta}) \geq \sup_{\theta \in \Theta} F_\infty(\theta) - 2\varepsilon.$$

Since ε is arbitrary, $\bar{\theta} \in F_\Theta(U)$.

We now identify the limit within $F_\Theta(U)$. Let $\theta^\dagger := \Pi_{F_\Theta(U)}(\theta^*)$, which is well-defined and unique since $F_\Theta(U)$ is a nonempty closed convex subset of Θ . For each $\sigma > 0$, optimality of $\hat{\theta}_\sigma$ gives

$$F_\sigma(\hat{\theta}_\sigma) \geq F_\sigma(\theta^\dagger).$$

Expanding F_σ yields

$$\langle \hat{\theta}_\sigma, U \rangle - \frac{1}{2\sigma\|Z\|} \|\hat{\theta}_\sigma - \theta^*\|^2 \geq \langle \theta^\dagger, U \rangle - \frac{1}{2\sigma\|Z\|} \|\theta^\dagger - \theta^*\|^2.$$

Rearranging,

$$\|\hat{\theta}_\sigma - \theta^*\|^2 \leq \|\theta^\dagger - \theta^*\|^2 - 2\sigma\|Z\|(\langle \theta^\dagger, U \rangle - \langle \hat{\theta}_\sigma, U \rangle).$$

Since $\theta^\dagger \in F_\Theta(U)$ maximizes $\langle \theta, U \rangle$ over Θ , the term in parentheses is non-negative, and hence

$$\|\hat{\theta}_\sigma - \theta^*\|^2 \leq \|\theta^\dagger - \theta^*\|^2 \quad \text{for all } \sigma > 0.$$

Let $\sigma_n \rightarrow \infty$ be any sequence such that $\hat{\theta}_{\sigma_n} \rightarrow \bar{\theta}$. By continuity of the norm,

$$\|\bar{\theta} - \theta^*\|^2 \leq \|\theta^\dagger - \theta^*\|^2.$$

Since $\bar{\theta} \in F_\Theta(U)$ and θ^\dagger is the unique minimizer of $\|\theta - \theta^*\|^2$ over $F_\Theta(U)$, it follows that $\bar{\theta} = \theta^\dagger$.

Because $\Theta \subset \mathbb{R}^d$ is compact, every sequence $\{\hat{\theta}_{\sigma_n}\}$ with $\sigma_n \rightarrow \infty$ admits a convergent subsequence, and the above argument shows that all such subsequences converge to θ^\dagger . Therefore,

$$\hat{\theta}_\sigma \rightarrow \Pi_{F_\Theta(U)}(\theta^*) \quad \text{a.s. as } \sigma \rightarrow \infty.$$

Finally, since $\hat{\theta}_\sigma \in \Theta$ for all σ and Θ is bounded, $\|\hat{\theta}_\sigma - \theta^*\|^2 \leq D^2$ almost surely. By dominated convergence,

$$\lim_{\sigma \rightarrow \infty} \mathbb{E} \|\hat{\theta}_\sigma - \theta^*\|^2 = \mathbb{E} \|\Pi_{F_\Theta(U)}(\theta^*) - \theta^*\|^2,$$

which completes the proof. \square

3.3.1 Proofs of results in Section 2.2.1

Proof of Lemma 2.5. Let $\Theta = \text{conv}\{v_1, \dots, v_K\} \subset \mathbb{R}^d$ with $d \geq 2$, and let $U \sim \text{Unif}(\mathcal{S}^{d-1})$. Since a linear functional attains its maximum over a polytope at a vertex,

$$\max_{\theta \in \Theta} \langle \theta, U \rangle = \max_{1 \leq i \leq K} \langle v_i, U \rangle.$$

If $d = 1$, then $\mathcal{S}^0 = \{-1, 1\}$ and the maximizer is trivially unique unless two vertices coincide, in which case the conclusion of the lemma still holds. We therefore assume $d \geq 2$ for the remainder of the proof. A tie between two distinct vertices v_i and v_j occurs at a direction $u \in \mathcal{S}^{d-1}$ if and only if

$$\langle v_i, u \rangle = \langle v_j, u \rangle \iff \langle v_i - v_j, u \rangle = 0.$$

Define the set of directions for which such a tie occurs by

$$B := \bigcup_{1 \leq i < j \leq K} \{u \in \mathcal{S}^{d-1} : \langle v_i - v_j, u \rangle = 0\}.$$

For any nonzero vector $a \in \mathbb{R}^d$, the set $\{u \in \mathcal{S}^{d-1} : \langle a, u \rangle = 0\}$ is a smooth $(d-2)$ -dimensional submanifold of \mathcal{S}^{d-1} and therefore has μ_{d-1} -measure zero. Since B is a finite union of such sets, it follows that $\mu_{d-1}(B) = 0$. As the uniform distribution on \mathcal{S}^{d-1} is absolutely continuous with respect to μ_{d-1} , we conclude that $\mathbb{P}(U \in B) = 0$.

Consequently, with probability one, the maximizer of $\langle \theta, U \rangle$ over Θ is unique and equals some vertex v_I . Moreover, this vertex is characterized by the condition $U \in \mathcal{N}_\Theta(v_I)$. \square

Proof of Lemma 2.7. By Lemma 2.5

$$R_\infty(\theta^*; \Theta_x) = \sum_j p_j \|v_j - \theta^*\|^2 = \sum_j p_j \|v_j\|^2 = \alpha_c p_2 + (1 + x^2)p_x,$$

where $\alpha_c := 1 + \frac{1}{c^2}$ and $p_j := \mathbb{P}(F_{\Theta_x}(U) = \{v_j\})$ for $j \in \{1, 2, x\}$. For any $U \sim \text{Unif}(\mathcal{S}^1)$,

$$\langle v_1, U \rangle = 0, \quad \langle v_2, U \rangle = \frac{U_1}{c} + U_2, \quad \langle v_x, U \rangle = xU_1 + U_2.$$

We now compute the vertex probabilities.

- p_2 . The event $\{S(U) = v_2\}$ is equivalent to the event $\{\langle v_2, U \rangle \geq \langle v_1, U \rangle, \langle v_2, U \rangle \geq \langle v_x, U \rangle\}$, which is equivalent to the event $\{\frac{U_1}{c} + U_2 \geq 0, U_1 \geq 0\}$. Let $R := \frac{U_2}{U_1}$, which is well defined almost surely. By Lemmas B.1 and B.2, the random variables R and $R \mid \{U_1 \geq 0\}$ are both standard Cauchy. It follows that

$$p_2 = \mathbb{P}(U_1 \geq 0, R \geq -\frac{1}{c}) = \frac{1}{2} \mathbb{P}(R \geq -\frac{1}{c}) = \frac{1}{4} + \frac{1}{2\pi} \arctan \frac{1}{c}.$$

- p_x . The event $\{S(U) = v_x\}$ is equivalent to the event $\{xU_1 + U_2 \geq 0, U_1 \leq 0\}$. Since

$$xU_1 + U_2 \geq 0 \iff U_1(x + R) \geq 0 \iff R \leq -x,$$

we have

$$p_x = \mathbb{P}(U_1 \leq 0, R \leq -x) = \frac{1}{2} \mathbb{P}(R \leq -x) = \frac{1}{4} - \frac{1}{2\pi} \arctan x.$$

□

Proof of Corollary 2.8. Taking $x = 0$ in Lemma 2.7 gives $\Theta_x = \Theta_L$, and if $x = \frac{1}{c}$ we obtain $\Theta_x = \Theta_S$. It follows immediately that with $\alpha_c = 1 + \frac{1}{c^2}$

$$\begin{aligned} R_\infty(\theta^*; \Theta_S) &= \alpha_c \left(\frac{1}{4} + \frac{1}{2\pi} \arctan \frac{1}{c} \right) + \alpha_c \left(\frac{1}{4} - \frac{1}{2\pi} \arctan \frac{1}{c} \right) = \frac{\alpha_c}{2}, \\ R_\infty(\theta^*; \Theta_L) &= \alpha_c \left(\frac{1}{4} + \frac{1}{2\pi} \arctan \frac{1}{c} \right) + \left(\frac{1}{4} - \frac{1}{2\pi} \arctan 0 \right) = \alpha_c \left(\frac{1}{4} + \frac{1}{2\pi} \arctan \frac{1}{c} \right) + \frac{1}{4}. \end{aligned}$$

□

3.3.2 Proofs of results in Section 2.2.2

Proof of Lemma 2.10. By Theorem 2.4, for each $\theta \in \Theta$,

$$R_\sigma(\theta; \Theta) \rightarrow R_\infty(\theta; \Theta).$$

We upgrade this pointwise convergence to uniform convergence on Θ . To this end, we first show that the family $\{R_\sigma(\cdot; \Theta) : \sigma > 0\}$ is uniformly bounded and equicontinuous on Θ . Throughout, write $D_\Theta := \text{diam}(\Theta) < \infty$. For any $\theta \in \Theta$ and $\sigma > 0$, both $\hat{\theta}_\sigma$ and θ belong to Θ , and therefore

$$\|\hat{\theta}_\sigma - \theta\| \leq D_\Theta,$$

and so $R_\sigma(\theta; \Theta) \leq D_\Theta^2$, from which it follows that the class is uniformly bounded. Next, fix $\sigma > 0$ and define

$$g_\sigma(\theta) := \|\Pi_\Theta(\theta + \sigma Z) - \theta\|^2.$$

For $\theta, \theta' \in \Theta$, set

$$a := \Pi_\Theta(\theta + \sigma Z) - \theta, \quad b := \Pi_\Theta(\theta' + \sigma Z) - \theta'.$$

Then

$$|g_\sigma(\theta) - g_\sigma(\theta')| = \|a\|^2 - \|b\|^2 \leq (\|a\| + \|b\|)\|a - b\|.$$

Since a, b are differences of points in Θ , we have $\|a\|, \|b\| \leq D_\Theta$. Since Θ is closed and convex, Π_Θ is 1-Lipschitz, and so

$$\|a - b\| \leq \|\Pi_\Theta(\theta + \sigma Z) - \Pi_\Theta(\theta' + \sigma Z)\| + \|\theta - \theta'\| \leq 2\|\theta - \theta'\|.$$

Hence, almost surely,

$$|g_\sigma(\theta) - g_\sigma(\theta')| \leq 4D_\Theta\|\theta - \theta'\|.$$

Taking expectations yields

$$|R_\sigma(\theta; \Theta) - R_\sigma(\theta'; \Theta)| \leq 4D_\Theta\|\theta - \theta'\|, \quad \text{for all } \sigma > 0.$$

Recall that a set of functions with common Lipschitz constant is uniformly equicontinuous. An identical argument applies with Π_Θ replaced by $\Pi_{F_\Theta(U)}$. Indeed, for each realization of U , $F_\Theta(U)$ is a nonempty closed convex subset of Θ , so $\Pi_{F_\Theta(U)}$ is well defined and $d(\theta, F_\Theta(U)) \leq D_\Theta$ for all $\theta \in \Theta$.

Let (σ_n) be any sequence with $\sigma_n \rightarrow \infty$. The family $\{R_{\sigma_n}(\cdot; \Theta)\}$ is uniformly bounded and equicontinuous on the compact set Θ , and converges pointwise to the continuous function $R_\infty(\cdot; \Theta)$. By the Arzelà–Ascoli theorem (see, e.g., [Dud02, Theorem 2.4.7]),

$$\sup_{\theta \in \Theta} |R_{\sigma_n}(\theta; \Theta) - R_\infty(\theta; \Theta)| \rightarrow 0.$$

Since this holds for every sequence $\sigma_n \rightarrow \infty$, we conclude that

$$\sup_{\theta \in \Theta} |R_\sigma(\theta; \Theta) - R_\infty(\theta; \Theta)| \rightarrow 0 \quad \text{as } \sigma \rightarrow \infty.$$

The claim follows from the inequality

$$\left| \sup_{\theta \in \Theta} R_\sigma(\theta; \Theta) - \sup_{\theta \in \Theta} R_\infty(\theta; \Theta) \right| \leq \sup_{\theta \in \Theta} |R_\sigma(\theta; \Theta) - R_\infty(\theta; \Theta)|.$$

□

Proof of Theorem 2.11. Let

$$\Delta := \sup_{\theta \in \Theta_S} R_\infty(\theta; \Theta_S) - \sup_{\theta \in \Theta_L} R_\infty(\theta; \Theta_L) > 0.$$

By Lemma 2.10, there exists σ_0 such that for all $\sigma \geq \sigma_0$,

$$\sup_{\theta \in \Theta_S} |R_\sigma(\theta; \Theta_S) - R_\infty(\theta; \Theta_S)| \leq \frac{\Delta}{3}, \quad \sup_{\theta \in \Theta_L} |R_\sigma(\theta; \Theta_L) - R_\infty(\theta; \Theta_L)| \leq \frac{\Delta}{3}.$$

Therefore, for all $\sigma \geq \sigma_0$,

$$\sup_{\theta \in \Theta_S} R_\sigma(\theta; \Theta_S) \geq \sup_{\theta \in \Theta_S} R_\infty(\theta; \Theta_S) - \frac{\Delta}{3} > \sup_{\theta \in \Theta_L} R_\infty(\theta; \Theta_L) + \frac{\Delta}{3} \geq \sup_{\theta \in \Theta_L} R_\sigma(\theta; \Theta_L),$$

which proves the claim. □

Proof of Lemma 2.12. For $x \in (0, 1/c)$, write $\Theta_x := \text{conv}\{v_1, v_2, v_x\}$ with $v_x = (x, 1)$. As shown in the proof of Lemma 2.7, the limiting risk takes the form

$$R_\infty(\theta; \Theta_x) = p_1^x \|\theta\|^2 + p_2 \|v_2 - \theta\|^2 + p_x \|v_x - \theta\|^2,$$

where

$$p_2 = \frac{1}{4} + \frac{1}{2\pi} \arctan \frac{1}{c}, \quad p_x = \frac{1}{4} - \frac{1}{2\pi} \arctan x, \quad p_1^x = 1 - p_2 - p_x.$$

For each x , the map $\theta \mapsto R_\infty(\theta; \Theta_x)$ is a convex quadratic function. Since Θ_x is compact and convex, its maximum is attained at an extreme point, and hence

$$\sup_{\theta \in \Theta_x} R_\infty(\theta; \Theta_x) = \max\{R_\infty(v_1; \Theta_x), R_\infty(v_2; \Theta_x), R_\infty(v_x; \Theta_x)\}.$$

Writing $\alpha_c := 1 + c^{-2}$, a direct calculation yields

$$\begin{aligned} R_\infty(v_1; \Theta_x) &= \alpha_c p_2 + p_x(1 + x^2), \\ R_\infty(v_2; \Theta_x) &= \alpha_c p_1^x + p_x(\frac{1}{c} - x)^2, \\ R_\infty(v_x; \Theta_x) &= p_1^x(1 + x^2) + p_2(\frac{1}{c} - x)^2. \end{aligned}$$

Evaluating these expressions gives

$$\sup_{\theta \in \Theta_a} R_\infty(\theta; \Theta_a) = \max\{1.324659, 1.306278, 0.808860\} = 1.324659,$$

and

$$\sup_{\theta \in \Theta_b} R_\infty(\theta; \Theta_b) = \max\{1.385120, 1.383614, 1.340221\} = 1.385120.$$

Since $a < b$ implies $\Theta_b \subset \Theta_a$, the desired strict inequality follows. \square

4 Conclusion

This work identifies a previously unrecognized failure mode of the constrained least squares estimator. We show that the risk of the LSE need not improve—and can in fact worsen—when the feasibility constraint is tightened, even when the constraint is compact, convex, and correctly specified. Within the Gaussian sequence model, we introduced the notion of risk reversal and constructed explicit examples in which a smaller nested constraint yields strictly worse performance than a larger one.

Importantly, this phenomenon arises at multiple levels. We establish risk reversal both pointwise, at fixed parameter values, and in a worst-case sense, where the supremum risk over the smaller feasible set exceeds that over the larger set. The latter shows that risk reversal is not a localized pathology, but can reflect a genuine degradation in global performance, underscoring its relevance for statistical practice.

Our analysis reveals that risk reversal is fundamentally geometric and non-local in nature. It results from the interaction between noise and the global structure of the constraint set, rather than from local curvature or asymptotic approximations around the true parameter. In particular, tightening a constraint can eliminate favorable geometric configurations and shift probability mass toward more distant faces or vertices of the feasible set, thereby increasing estimation error.

Notably, these effects arise in the Gaussian sequence model, one of the most canonical settings for constrained estimation, where the LSE coincides with the maximum likelihood estimator and the noise is light-tailed. From this perspective, the Gaussian sequence model serves as a conservative testbed: risk reversal must stem from genuinely global geometric interactions between the constraint and the noise, rather than from model misspecification or high-dimensional effects.

More broadly, these results suggest that the behavior of projection-based estimators can depend sensitively on how noise interacts with constraint geometry, and that tighter feasibility constraints are not uniformly beneficial. While a general characterization appears intractable, we show that progress is possible for restricted classes of sets, providing sufficient geometric conditions for risk reversal for convex polytopes. Extending these ideas to broader classes of convex constraints remains an important direction for future work.

Acknowledgments

I am grateful to P. Rigollet for many helpful discussions, and I thank S. Kotekal and M. Neykov for insightful feedback on an early draft. This work was supported by funding from the Eric and Wendy Schmidt Center at the Broad Institute of MIT and Harvard.

References

[AJPU25] Liviu Aolaritei, Michael I Jordan, Reese Pathak, and Annie Ulichney. Revisiting mean estimation over ℓ_p balls: Is the MLE optimal? *arXiv preprint arXiv:2506.10354*, 2025.

[ALMT14] Dennis Amelunxen, Martin Lotz, Michael B McCoy, and Joel A Tropp. Living on the edge: Phase transitions in convex programs with random data. *Information and Inference: A Journal of the IMA*, 3(3):224–294, 2014.

[BDK⁺22] Olivier J Bousquet, Amit Daniely, Haim Kaplan, Yishay Mansour, Shay Moran, and Uri Stemmer. Monotone learning. In *Conference on Learning Theory*, pages 842–866. PMLR, 2022.

[BM93] Lucien Birgé and Pascal Massart. Rates of convergence for minimum contrast estimators. *Probability Theory and Related Fields*, 97(1):113–150, 1993.

[Cha14] Sourav Chatterjee. A new perspective on least squares under convex constraint. *The Annals of Statistics*, 42(6):2340 – 2381, 2014.

[Dud02] R. M. Dudley. *Real Analysis and Probability*. Cambridge Studies in Advanced Mathematics. Cambridge University Press, 2 edition, 2002.

[FG19] Billy Fang and Adityanand Guntuboyina. On the risk of convex-constrained least squares estimators under misspecification. *Bernoulli*, 25(3):2206–2244, 2019.

[Han23] Qiyang Han. Noisy linear inverse problems under convex constraints: Exact risk asymptotics in high dimensions. *The Annals of Statistics*, 51(4):1611–1638, 2023.

[Joh19] Iain M. Johnstone. *Gaussian Estimation: Sequence and Wavelet Models*. 2019. Draft.

[KGGS24] Gil Kur, Fuchang Gao, Adityanand Guntuboyina, and Bodhisattva Sen. Convex regression in multidimensions: Suboptimality of least squares estimators. *The Annals of Statistics*, 52(6):2791–2815, 2024.

[KPR23] Gil Kur, Eli Puterman, and Alexander Rakhlin. On the variance, admissibility, and stability of empirical risk minimization. *Advances in Neural Information Processing Systems*, 36:37527–37539, 2023.

[KRG20] Gil Kur, Alexander Rakhlin, and Adityanand Guntuboyina. On suboptimality of least squares with application to estimation of convex bodies. In *Conference on Learning Theory*, pages 2406–2424. PMLR, 2020.

[MH20] Zakaria Mhammedi and Hisham Husain. Risk-monotonicity via distributional robustness, 2020.

[Ney23] Matey Neykov. On the minimax rate of the gaussian sequence model under bounded convex constraints. *IEEE Transactions on Information Theory*, 69(2):1244–1260, 2023.

[Nol95] Dominikus Noll. Directional differentiability of the metric projection in hilbert space. *Pacific Journal of Mathematics*, 170(2):567–592, 1995.

[OH16] Samet Oymak and Babak Hassibi. Sharp mse bounds for proximal denoising. *Foundations of Computational Mathematics*, 16(4):965–1029, 2016.

[OTH13] Samet Oymak, Christos Thrampoulidis, and Babak Hassibi. The squared-error of generalized lasso: A precise analysis. In *2013 51st Annual Allerton Conference on Communication, Control, and Computing (Allerton)*, pages 1002–1009. IEEE, 2013.

[Owe80] Donald Bruce Owen. A table of normal integrals: A table. *Communications in Statistics-Simulation and Computation*, 9(4):389–419, 1980.

[PN25] Akshay Prasadan and Matey Neykov. Some facts about the optimality of the lse in the gaussian sequence model with convex constraint. *IEEE Transactions on Information Theory*, 2025.

[Sha16] Alexander Shapiro. Differentiability properties of metric projections onto convex sets. *Journal of Optimization Theory and Applications*, 169(3):953–964, 2016.

[Tsy09] Alexandre B. Tsybakov. *Introduction to Nonparametric Estimation*. Springer Series in Statistics. Springer, New York, 2009.

[VdV00] Aad W Van der Vaart. *Asymptotic statistics*, volume 3. Cambridge university press, 2000.

[VML20] Tom Julian Viering, Alexander Mey, and Marco Loog. Making learners (more) monotone. In *International Symposium on Intelligent Data Analysis*, pages 535–547. Springer, 2020.

[WFW20] Yuting Wei, Billy Fang, and Martin J. Wainwright. From Gauss to Kolmogorov: localized measures of complexity for ellipses. *Electron. J. Stat.*, 14(2):2988–3031, 2020.

[Zar71] Eduardo H Zarantonello. Projections on convex sets in hilbert space and spectral theory: Part i. projections on convex sets: Part ii. spectral theory. In *Contributions to nonlinear functional analysis*, pages 237–424. Elsevier, 1971.

[Zha13] Li Zhang. Nearly optimal minimax estimator for high-dimensional sparse linear regression. *The Annals of Statistics*, 41(4):2506–2537, 2013.

Appendix

A Background on Owen’s T-function

In Theorem 3.1, our risk expressions involve *Owen’s T-function* [Owe80]. We recall here its definition and basic properties. For $h, a \in \mathbb{R}$, let

$$T(h, a) := \phi(h) \int_0^a \frac{\phi(hz)}{1+z^2} dz.$$

The function T satisfies the following basic identities:

$$T(\infty, a) = 0, \quad T(h, 0) = 0, \quad T(0, a) = \frac{1}{2\pi} \arctan a, \quad T(h, \infty) = \frac{1}{2} \Phi(-h), \quad T(h, -a) = -T(h, a),$$

where expressions involving infinite or zero arguments are understood in the sense of limits. We also make use of the following Gaussian integral identity.

Proposition A.1 ([Owe80]). *Let $a, b \in \mathbb{R}$ and write $r_{a,b} := \frac{a}{\sqrt{1+b^2}}$. For any $m \geq 0$,*

(i)

$$\begin{aligned} \int_0^m \phi(z)\Phi(a+bz)dz &= T\left(m, \frac{r_{a,b}}{m}\right) + T\left(r_{a,b}, \frac{m}{r_{a,b}}\right) - T\left(m, \frac{a}{m} + b\right) \\ &\quad - T\left(r_{a,b}, b + \frac{m}{a}(1+b^2)\right) + \Phi(m)\Phi(r_{a,b}) - \frac{1}{2}\Phi(r_{a,b}) + T(r_{a,b}, b). \end{aligned}$$

(ii) For any $b \in \mathbb{R}$ and $m \geq 0$,

$$\int_0^m \phi(z)\Phi(bz)dz = \frac{1}{2}\Phi(m) - \frac{1}{4} - T(m, b) + \frac{1}{2\pi} \arctan b.$$

In particular, this identity is obtained by taking the limit $a \rightarrow 0$ in (i).

(iii) For $m \geq 0$,

$$\begin{aligned} \int_0^m z\phi(z)\phi(a+bz)dz &= \frac{1}{1+b^2}\phi(r_{a,b})\left[\phi(br_{a,b}) - \phi\left(m\sqrt{1+b^2} + br_{a,b}\right)\right] \\ &\quad + \frac{ab}{(1+b^2)^{3/2}}\phi(r_{a,b})\left[\Phi(br_{a,b}) - \Phi\left(m\sqrt{1+b^2} + br_{a,b}\right)\right]. \end{aligned}$$

B Ratios of coordinates of a uniform random vector

We collect two elementary facts on ratios of coordinates of a uniform random vector on the unit circle, used in the proof of Lemma 2.7.

Lemma B.1. Let $U = (U_1, U_2) \sim \text{unif}(\mathcal{S}^1)$ and define $R := \frac{U_2}{U_1}$. Since $\mathbb{P}(U_1 = 0) = 0$, R is well defined almost surely. Then $R \sim \text{Cauchy}(0, 1)$.

Proof. Let $Z = (Z_1, Z_2) \sim N(0, I_2)$, then by rotational invariance $U \stackrel{d}{=} \frac{Z}{\|Z\|}$. Then, using a standard fact about the ratio of i.i.d. standard normals, we have

$$\frac{U_2}{U_1} = \frac{Z_2}{Z_1} \sim \text{Cauchy}(0, 1)$$

□

Lemma B.2. Let $U = (U_1, U_2) \sim \text{unif}(\mathcal{S}^1)$ and define $R := \frac{U_2}{U_1}$. Since $\mathbb{P}(U_1 = 0) = 0$, R is well defined almost surely. Then $R|U_2 > 0 \sim \text{Cauchy}(0, 1)$.

Proof. Let $Z = (Z_1, Z_2) \sim N(0, I_2)$, then by rotational invariance $U \stackrel{d}{=} \frac{Z}{\|Z\|}$. Let $(X, R) := (Z_1, \frac{Z_2}{Z_1})$ and consider the change of variables $(x, r) \mapsto (z_1, z_2) = (x, xr)$. The Jacobian matrix is

$$\begin{bmatrix} \frac{\partial z_1}{\partial x} & \frac{\partial z_1}{\partial r} \\ \frac{\partial z_2}{\partial x} & \frac{\partial z_2}{\partial r} \end{bmatrix} = \begin{bmatrix} 1 & 0 \\ r & x \end{bmatrix},$$

so the determinant of the Jacobian is $J(x, r) = x$. The joint density of (X, R) is

$$f_{X,R}(x, r) = f_{Z_1, Z_2}(x, xr)|J(x, r)| = \frac{|x|}{2\pi} \exp\left(-\frac{(1+r^2)x^2}{2}\right).$$

Conditioning on $U_1 \geq 0$ is the same as conditioning on $Z_2 > 0$, which corresponds to the region $\{xr > 0\}$. We get

$$\begin{aligned}
f_{R|Z_2>0}(r) &= \frac{1}{\mathbb{P}(Z_2 > 0)} \int_{\{x: xr > 0\}} f_{X,R}(x, r) dx \\
&= 2 \int_{\{x: xr > 0\}} \frac{|x|}{2\pi} \exp\left(-\frac{(1+r^2)x^2}{2}\right) dx \\
&= \int_0^\infty \frac{x}{2\pi} \exp\left(-\frac{(1+r^2)x^2}{2}\right) dx \\
&= \frac{1}{\pi(1+r^2)},
\end{aligned}$$

which is the standard Cauchy density. \square